plate was subconfluent, cells were treated with 0.25% trypsin/0.5 mM EDTA solution (both from Invitrogen, Tokyo, Japan) and replated at a density of 5×10^3 cells/ml.

All of the cells were maintained in a humidified incubator at 37° C and 5% CO_2. PDLs were calculated using the formula: PDL= log (cell output/input)/log2. At the starting cultivation, PDLs of UCBTERT-21, UCB408E6E7 TERT-33, UE6E7T-3, and UBE6T-6 were 42, 67, 60, and 56, respectively. The doubling time of the UCB408E6E7T-33 cell was 1.5 d, and that of UCBTERT-21, UE6E7T-3, or UBE6T-6 was 2.6, 2.0, or 4.0 days, respectively.

Measurement of chromosome number and fluorescence in situ hybridization. Metaphase chromosome spreads for measurement of chromosome number and fluorescence in situ hybridization (FISH) were prepared from exponential growing cells at various PDL. The cells were treated in a hypotonic solution after exposure to 0.06 μg/ml colcemid (Invitrogen, Carlsbad, CA) for 2 h and fixed in methanol/acetic acid (3:1). The cells were spread on a microscope slide.

To count the number of chromosomes, the cells were stained with DAPI (4′-6-diaminido-2-phenylindol; Vector Laboratories, Inc. Burlingame, CA) and examined under an Axioplan II imaging microscope (Carl Zeiss, GmbH) equipped with Leica QFISH software (Leica Microsystems Holding, UK). To examine statistically significant chromosome numbers, we have allowed ±1 deviation and 50–100 metaphase spreads were scored for each assay.

Painting probes specific for chromosome 13 (XCP13-kit, FITC; MetaSystems, GmbH) and chromosome 17 (XCP17-kit; Texas Red) (MetaSystems GmbH, Altlussheim, Germany), and multicolor probes (mFISH-24Xcyte-kit, DAPI, FITC, TexasRed, Cy3, Cy5, and DEAC; MetaSystems GmbH) were used for FISH analysis. FISH was performed according to the manufacture's protocol (MetaSystems GmbH). Briefly, both the metaphase chromosome spread and the probe were denatured with 0.07 N NaOH or 70% formamide, hybridized at 37° C for 1–4 d, and counterstained with DAPI. FISH images were captured and analyzed on the Zeiss Axio Imaging microscope (Carl Zeiss Microimaging GmbH, Jena, Germany) with Isis mBAND/mFISH imaging Software (MetaSystems GmbH).

CGH analysis. Hybridization was carried out with the BAC Array (MAC ArrayTM Karyo 4000 Component, Macrogen Co., Rockville, MD) by the Hybstation (Genomic Solutions, Ann Arbor, MI). Briefly, test DNAs, which were isolated using an isolation kit (Amersham BioSciences, Little Chalfont, UK) and Spin Column (QIAGEN Co., Tokyo, Japan), and reference DNAs (Promega Co., Madison, WI), were labeled, respectively, with Cy3 or Cy5 (BioPrimer DNA Labeling System, Invitrogen Co.), precipitated together with ethanol in the presence of Cot-1 DNA, redissolved in a hybridization mixture (50% formamide, 10% dextran sulfate, 2xSSC, 4% sodium dodecyl sulfate [SDS], pH 7), and denatured at 75° C for 10 min. After incubation at 37° C for 30 min, each mixture was applied to an array slide and incubated at 42° C for 48–72 h. After hybridization, the slides were washed in a solution of 50% formamide—2× SSC (pH 7.0) for 15 min at 50° C, in 2× SSC—0.1% SDS for 15 min at 50° C, and in a 100-mM sodium phosphate buffer containing 0.1% Nonidet P-40 (pH 8) for 15 min at room temperature, then scanned with GenePix4000A (Axon Instruments, Union City, CA). Acquired images were analyzed with MacViewer (Macrogen Instruments).

Differentiation ability. To evaluate the differentiation potential of each cell line, cells were cultured on a coverslip in each induction medium, that is, hMSC Differentiation BulletKit-Adipogenic (PT-3004, Cambrex BioScience, Inc., Walkersville, MD) for adipocyte and NPMM Bullet kit (NPMM™ BulletKit (B3209, Cambrex BioScience) for neural progenitor cells. For osteoblast, cells were treated with 0.1 μM dexamethasone (Sigma Chemical Co., St. Louis, MO), 50 μg/ml L-ascorbic acid (Sigma Chemical), and 10 mM β-glycerophosphate (Sigma Chemical) in the PLUSOID-M medium (Med-Shirotori Co.) or the POWER-EDBY10 medium (Med-Shirotori Co.) of culture medium.

After 2–4 wk, the cells were washed in phosphate-buffered saline (PBS), fixed in 4% paraformaldehyde in PBS and stained with Oil Red-O (Sigma Chemical) for detection of adipocyte, and with alkaline phosphatase staining solution containing 0.25 mg/ml naphthol AS-BI phosphate and 0.25 mg/ml Fast violet LB salt for detection of alkaline phosphatase-positive osteoblast. In immunostaining for neuron-like cells, the cells fixed with paraformaldehyde were permeabilized with methanol at −20° C for 10 min and stained with an anti-IIIβ tubulin antibody (Sigma Chemical) or anti-neurofilament antibody NF-200 (Sigma Chemical) and Texas Red-anti-mouse IgG (Southern Biotechnology Associates, Inc., Birmingham, AL) as previously described (Takeuchi et al. 1990).

Results

Changes in chromosomal number in human mesenchymal stem cell lines in prolonged culture. Immortalization of cultured cells frequently induces an abnormal chromosome number as shown in cancer cells (Duensing et al. 2000; Munger et al. 2004; Patel et al. 2004), especially at higher frequency in long-term culture. We therefore examined four cell lines, human mesenchymal stem cell (hMSC) lines immortalized with combinations of bmi-1, E6, E7, and/or hTERT genes, for chromosome instability by counting metaphase chromosomes.

All of the lines were diploid, each containing 46 up to 40 PDL including the PDL numbers of nontransfecting original MSCs (Takeda et al. 2004; Mori et al. 2005; Terai et al. 2005). For UCBTERT-21 cell, no further changes in chromosome number have been observed up to date (for PDL 133) as shown in Fig. 1*A* and *B*. In contrast, although the UBE6T-6 cell and the UE6E7T-3 cell were near diploid, both cells exhibited considerable variation in chromosome number from PDL 70 after the culture started. For example, when the assay of UE6E7T-3 cells start at PDL 62 in culture, 90% of cell population had 46 chromosomes, but the population decreased with prolonged culturing and a population containing 44 chromosomes became dominant (43% of cell populations) at PDL 147 (Fig. 1*E*, *F*). A similar variation was also observed in UBE6T-6 cells (Fig. 1*C*, *D*).

To ascertain whether or not the changes observed were induced by transfection with HPV16E6E7, we assayed the chromosome numbers of UCB408E6E7TERT-33 cell in prolonged culture. The cell line showed similar chromosomal changes to those of the UE6E7T-3 cell, the rate of which was more rapid. At day 2 after culture by us changes became evident (PDL 68), the UCB408E6E7TERT-33 cells consisted of two distinct populations concerning chromosome number (near diploid [24%] and near tetraploid [53%]), shown in Fig. 1*G*. However, the near diploid population was unstable and decreased gradually. At PDL 81, the population became only near tetraploid, 80% of the

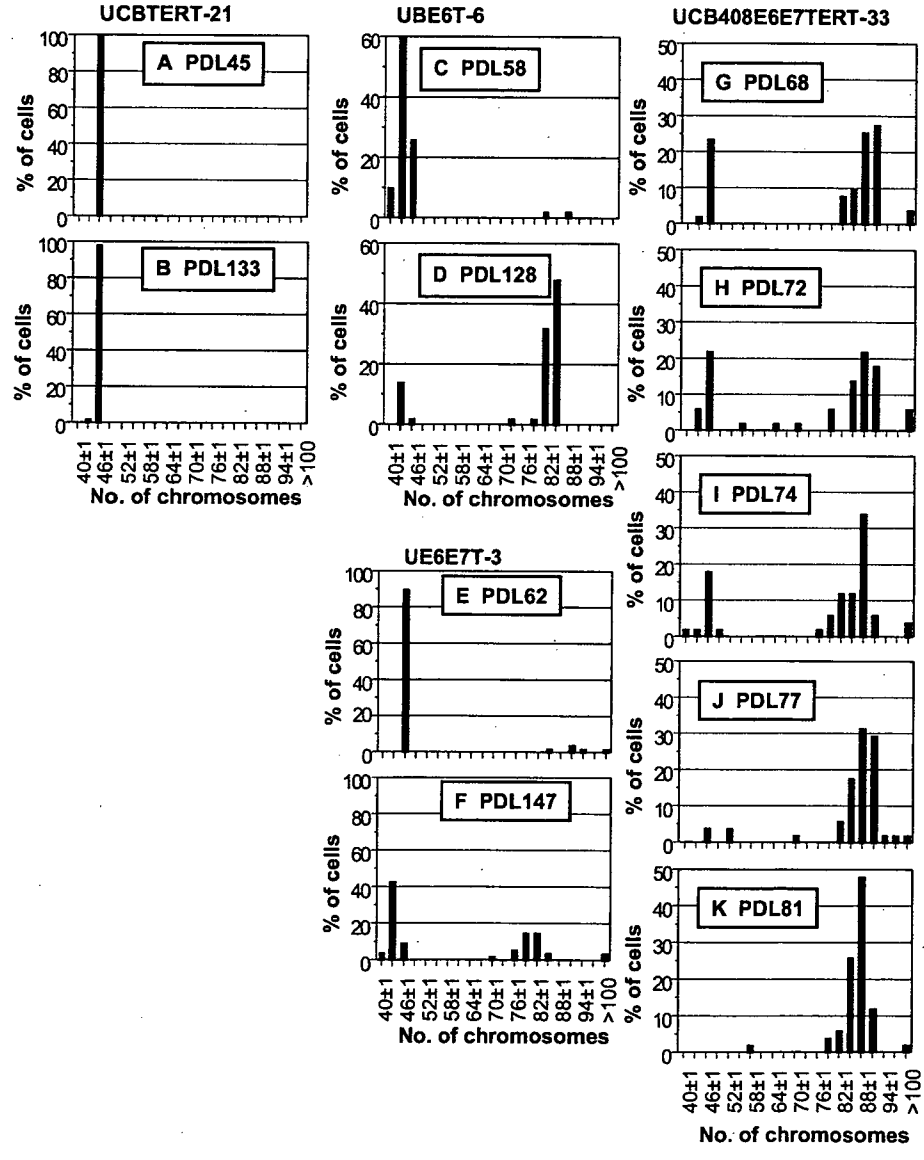

Figure 1. Changes in chromosomal numbers in prolonged cultures of four hMSC cell lines. (*A–K*) The chromosomal numbers at various culture stages were counted by DAPI staining. (*A*, *B*), (*C*, *D*), (*E*, *F*), and (*G–K*) represent the chromosomal numbers from UCBTERT-21, UBE6T-6, UE6E7T-3, and UCB408E6E7TERT-33, respectively. To examine statistically significant chromosomal numbers, we have allowed ±1 deviation, and 50–100 metaphase spreads were examined for each assay. *Note* the changes in chromosomal number from near 2*n* to near 4*n* in prolonged culture.

cells contain 85–92 chromosomes (Fig. 1*K*). The results indicate that UCBTERT-21 is relatively stable in chromosome number, whereas each of the oncogene-immortalized cells (UE6E7T-3, UBE6T-6, and UCB408E6E7TERT-33 cell) were unstable in chromosome numbers, which altered substantially during prolonged culture.

We next applied FISH and CGH analysis to characterize the chromosomal aberrations of the cell lines. All of the four cell lines passed for PDL 50 before examination by FISH. mFISH analysis of the UCBTERT-21 cell at PDL 52 showed normal chromosome composition (Fig. 2*A* and *B*) as observed in non-immortalized cells. The UBE6T-6 cell containing 43–45 chromosomes demonstrates losses of chromosome 13, 16, and 19 (marginal variation in chromosome 4 was observed among cells), but keeps on proliferating in chromosome number of 43–45 (Fig. 2*D*, *E*). In contrast, the UCB408E6E7TERT-33 cell showed more heterogeneity in chromosome composition with intrachromosomal and interchromosomal aberrations (data not shown). However, by mFISH analysis we were able to detect nonrandom losses of chromosome 13 in three cell lines except the UCBTERT-21 cell line. This was also confirmed by pFISH analysis using the probes specific for chromosome 13 and chromosome 17 (Fig. 2*C*, *F*). More than 97% of UCBTERT-21 cells showed two copies for chromosome 13, indicating the stability of the chromosomes in the cell line (Fig. 2*G*). The UE6E7T-3 and the UBE6T-6 cell lines with chromosome numbers of 43–45 showed only one copy of chromosome 13 in 76% of UE6E7T-3 cells and 86% of UBE6T-6 cells, respectively (Fig. 2*I*, *J*). A similar loss of chromosome 13 was also observed in 70% of UCB408E6E7TERT-33 cells, which showed three copies of chromosome 13 in near tetraploid (Fig. 2*H*). Other chromosomes, for example chromosome 17, were contained in the UCBTERT-21 and UBE6T-6 cell lines (Fig. 2*C*, *F*).

Furthermore, a significant nonrandom loss of chromosome 13 at the single cell-level observed by FISH was examined by array CGH, which samples the entire cell population. Figure 3 shows the array CGH profiles from early (*blue spots*) and late (*red spots*) stages of proliferating of each cell line. The UCBTERT-21 cell did not show any detectable differences in array CGH profiles between early and late stages (Fig. 3*A*). Although the loss of chromosome 13 had already occurred at early stages in the UBE6T-6 and the UCB408E6E7TERT-33 cell lines, in addition to the losses of chromosomes 4, 9, and 16 (Fig. 3*B*, *D*), in UE6E7T-3 the loss appeared between PDL 78 to 101 with loss of chromosome 16. The most compelling observation was that all three cell lines revealed a consistent whole loss of chromosome 13. These data are consistent with the results observed by FISH analysis. From these results, we

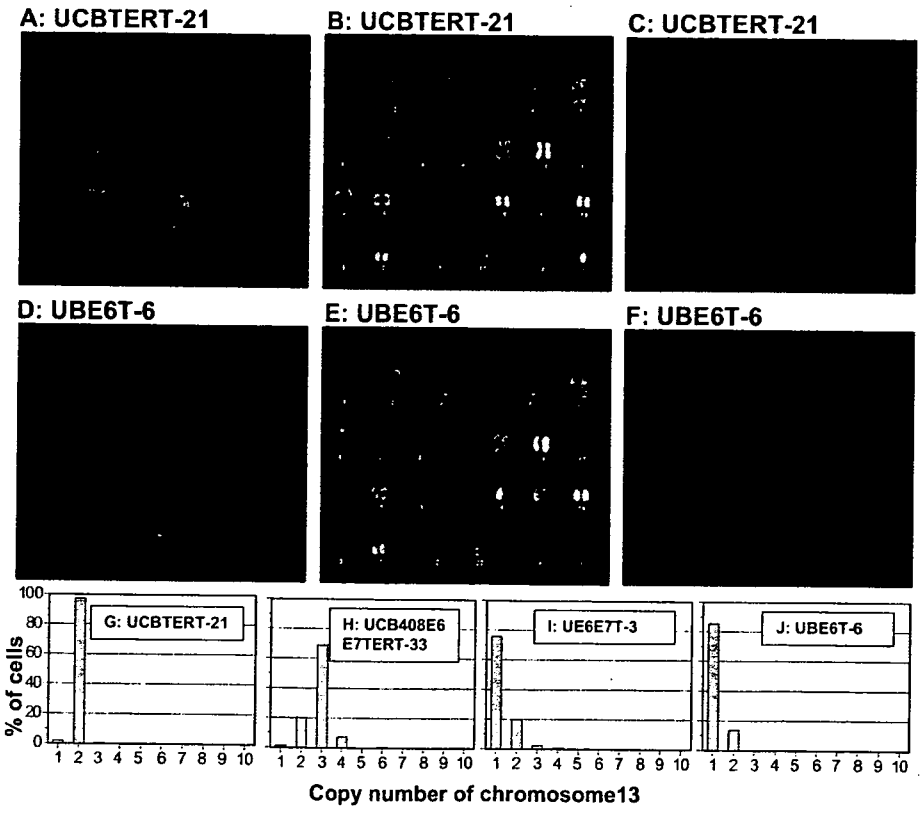

Figure 2. FISH analysis of human mesenchymal stem cell (hMSC) lines immortalized with hTERT alone, hTERT plus bm-1, HPVE6 or with hTERT plus HPVE6/E7. Multicolor FISH images of metaphase spreads (*A*, *D*), their karyotypes (*B*, *E*), and painting FISH images using DNA probes specific for chromosome 13 (*green*) and 17 (*red*) (*C*, *F*) of UCBTERT-21 (*A*, *B*, *C*) and UBE6T-6 (*D*, *E*, *F*). Quantity of chromosome 13 copy numbers in four cell lines (*G–J*). FISH signals were counted in 120~200 metaphase spreads plus interphase nuclei. UCBTERT-21 cells contained two copies of chromosome 13 and 17, and showed normal human karyotype, whereas other cells lost one copy of chromosome 13.

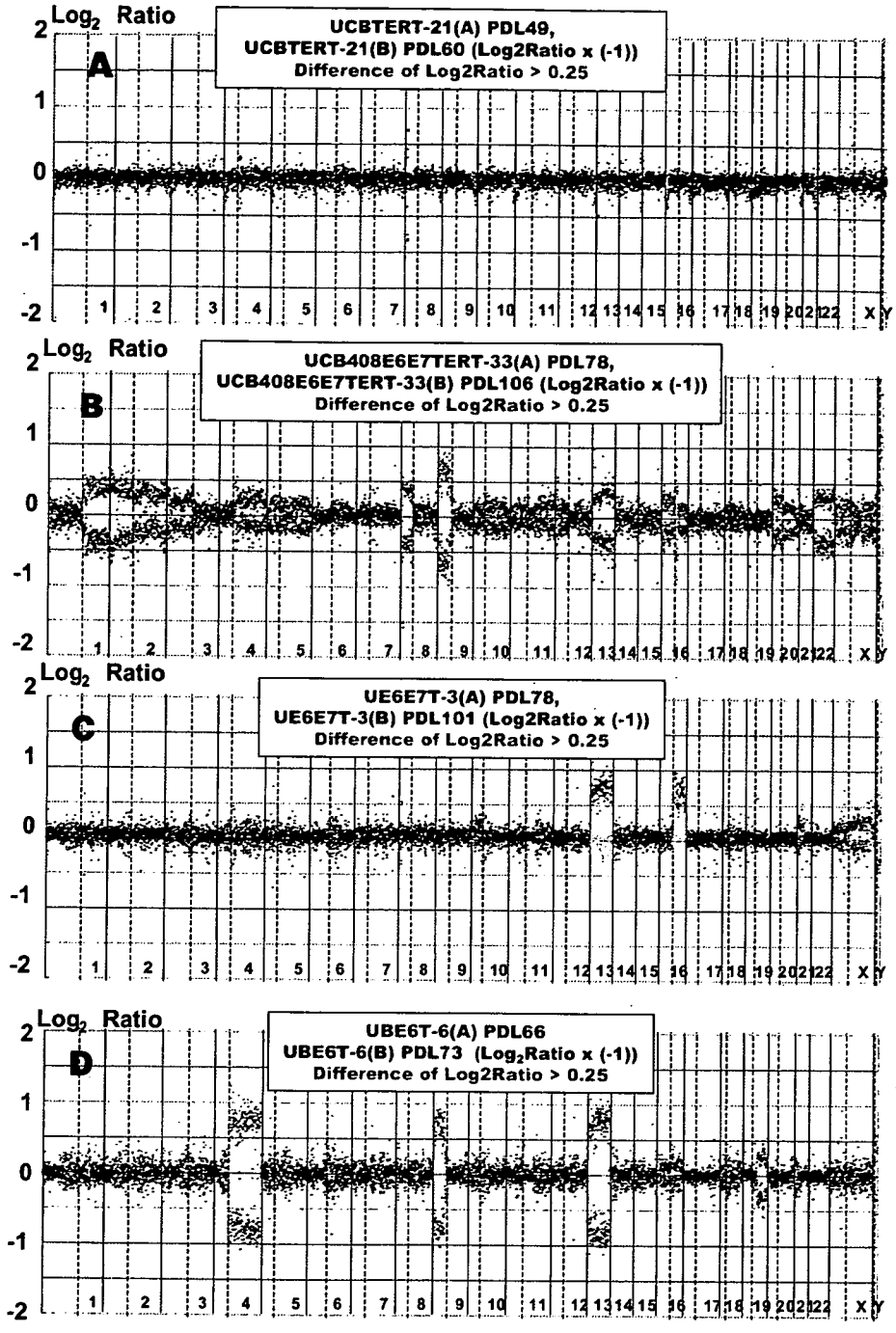

Figure 3. Array CGH profiles performed on four immortalized human mesenchymal stem cell lines at selected PDL. For each *panel*, the *X*-axis represents the 22 autosomes, the *X* and *Y* chromosomes, and the *Y*-axis shows the $\log_2$ of the fluorescence intensity ratio (cy3 [hMSCs]/cy5 [normal cell]) of all spots of the chromosome. Values above 0 (*red spots*) or values below 0 (*blue spots*) signify a loss of chromosome (chromosome regions). *Blue spots* in each *panel* indicate the $\log_2$ ratios observed at early stage in the culture of each cell line, which are overlaid with *red spots* indicated at the late stage. *Green spots* indicate the difference in value between *blue spots* and *red spot*. *Note* that in the UE6E7T-3 cell line, one copy of chromosome 13 and 16 were lost between PDL 78 and 101.

concluded that only hTERT-mediated immortalization induced little change in the chromosome numbers and chromosome structures of mesenchymal stem cells, but immortalization with Bmi-1, E6, and E7 in addition to hTERT results in chromosome instability.

Differentiation potential into lineages of immortalized mesenchymal stem cell lines. It has been reported that mesenchymal stem cells have the extensive potential to differentiate into multiple cell lineages including osteoblast, chondrocytes, adipocytes (Pittenger et al. 1999), cardiac myocytes (Makino et al. 1999), and neural cells (Pacary et al. 2006; Wislet-Gendebien et al. 2005). To evaluate whether chromosome instability of these cell lines in prolonged culture affects differentiation, cells of each cell line were stimulated in each induction medium for 2 to 4 wk. In

adipocyte-specific culture medium, all cell lines accumulated lipid-rich vacuoles in their cytoplasm within 2 wk, which were made evident by Oil Red-O staining. In particular, the UE6E7T-3 cell line showed a greater adipogenetic ability among the four cell lines (Fig. 4*Ab*). In osteoblast induction medium for 2 wk, UCB408E6E7 TERT-33 cells showed a marked increase in alkaline phosphatase expression, a marker of osteoblast, compared with those in the three other cell lines (Fig. 4*Ad*). In addition, UBE6T-6 cells in neuron induction medium reduced proliferation and displayed marked changes in morphology from being a flat-polygonal shape to taking on the characteristic neuron-like shape in which the cells develop long branching processes. Moreover, in comparing the expression patterns of characteristic neural antigens, i.e., neurofilament, III-β-tubulin, before and after induction (28 d), the pseudo-neural shaped cells showed apparent increases in immunoreactivity to both antibodies (Fig. 4*Af, Ah*),

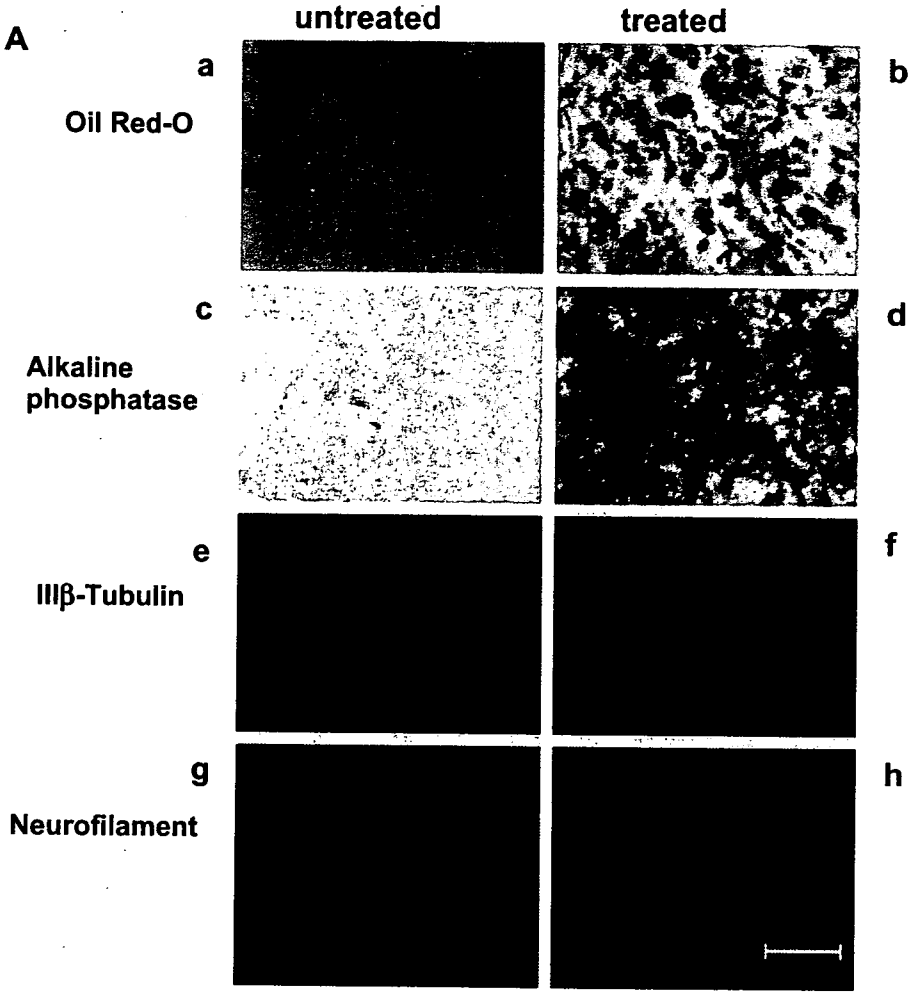

Figure 4. Differentiation potential of immortalized human mesenchymal stem cell lines into adipogenic, osteogenic, and neurogenic lineages. Adipogenesis was indicated by the accumulation of lipid stained with Oil Red-O (*Aa* and *Ab*, UE6E7T-3 cell line). Osteogenesis is indicated by the increase in alkaline phosphatase (*Ac* and *Ad*, UCB408E6E7TERT-33 cell line). Neurogenesis was shown by staining with two kinds of monoclonal antibodies to IIIβ-tubulin and neurofilament, and by shape changes of cell (*Ae–Ah*, UBE6T-6 cell line). *B*, Comparison of the differentiation potential of four cell lines whose responses to stimuli into differentiation were diverse among the cell lines. − and + indicate a response similar to an untreated cell and a weak positive response. +++ indicates a strong response shown by images of treated cells in Fig. 4*A*. (*Bar* indicates 20 μm).

B

	UCBTERT-21	UCB408E6E7TERT-33	UE6E7T-3	UBE6T-6
Oil Red-O	+	++	+++	+
Alkarine phosphatase	+	+++	+	+
IIIβ- Tubulin	-	+	+/-	+++
Neurofilament	-	++	-	++

whereas such changes were not evident with the flat-shaped cells before induction (Fig. 4*Ae*, *Ag*). Additionally, such cells did not undergo such differentiation in culture medium when cultured for as long as 30 d, although faint staining was observed. Figure 4*B* shows the overall results of differentiation potential of the four cell lines into adipogenic, osteogenic, and neurogenic lineages. These immortalized mesenchymal stem cell lines retained the ability to differentiate into three lineages, although among cell lines there are significant variations in response to lineage-specific induction.

Discussion

Attempts to clarify the mechanisms for extending the lifespan of tumor cells have been made for many years, and several genes that have effects on cellular proliferation and survival have become clear (Munger et al. 2002) in addition to the elucidation that the majority of tumor cells express telomerase (hTERT; Armanios et al. 2005). The goal of one of the series of our studies has been to establish cell lines with long lifespan and with parental properties, on the basis of genotypic and phenotypic characterizations, for application to cell-based therapy. We previously established several cell lines (Takeda et al. 2004; Mori et al. 2005; Terai et al. 2005), and the present study demonstrated that UCBTERT-21, the immortalized cell line derived from human umbilical cord blood-derived MSCs with hTERT, has a normal karyotype and has an extended lifespan by at least 133 population doublings, and has the differentiation potential into the adipocyte or osteoblast similar to parental MSCs (Terai et al. 2005), although the potential was weak but clearly positive in this study. The specific environmental cues to initiate the differentiation of hMSCs are not yet clear.

UCBTERT-21 immortalized with hTERT alone can be prolonged without inhibition of the $p16^{INK4A}$/RB pathway (Terai et al. 2005), the result of which is in agreement with reports that hTERT alone significantly extends the lifespan of human fibroblasts, epithelial, and endothelial cells (Bodnar et al. 1998; Chang et al. 2005), without the requirement for molecular alterations in p53/p21 and pRB/$p16^{INK4A}$ pathways (Milyavsky et al. 2003). However, other researchers have indicated that inactivation of the RB/p16 pathway by E7, or downregulation of p16 expression, in addition to increasing telomerase activities, is necessary for expanding the lifespan of human keratinocytes (Dickson et al. 2000; Kiyono et al. 1998). Thus, the possibility that a telomere-independent barrier may operate to prevent immortalization according to cell types has been indicated.

UCB408E6E7TERT-33, UE6E7T-3, and UBE6T-6 are hMSC-clones immortalized with HPV16E6/E7 or polycomb group oncogene Bmi-1, in combination with hTERT. Immortalization of human keratinocyte in vitro using virus-derived oncogenes such as E6 and E7 is based on initial inactivation of the p53 and/or Rb pathways, which are essential for controlling cell cycle progression in response to DNA damage or after induction tetraploidy; therefore, this gene transduction induces chromosomal abnormalities (Solinas-Toldo et al. 1997; Duensing et al. 2002; Patel et al. 2004; Schaeffer et al. 2004). The cell lines used in this study became completely immortal, yet underwent dynamic changes in their chromosome numbers in prolonged culture. Near diploid population in early passage of UCB408E6E7 TERT-33 became near-tetraploid population with prolonged culture without the appearance of intermediate populations (60–70 chromosomes/cell), and thereafter gave rise to a population having smaller numbers of chromosomes than tetraploid. Similar patterns existed, although at a slower rate, in UBE6T-6 cells and UE6E7T-3. These results suggest that HPVE6 and E7 proteins cause tetraploidy that precedes the chromosomal aberration to aneuploid in E6/E7-immotalized hMSCs, as is currently shown in several lines of evidence. For example, in vitro experiments in human cell lines (N/TERT-1 keratinocytes and HeLa cells) demonstrate that chromosome nondisjunction yields tetraploid rather than aneuploid, and that aneuploid may develop through chromosomal loss from tetraploid, although the mechanistic basis for the tetraploid formation still remains to be elucidated (Shi et al. 2005). This is also suggested from evidence that high frequency of tetraproidy is present with aneuploidy in human tumors (Olaharski et al. 2006; Sen 2000). A distinct pattern of aneuploid became apparent using dual-probe FISH and CGH analyses, in which UCB408E6E7TERT-33 cells predominantly exhibited triploid 13 and tetraploidy 17 together with other chromosomal changes as shown in Figs. 2 and 3. However, surprisingly, the loss of one copy of chromosome 13 was also seen in 70–80% of diploid UE6E7T-3 and diploid UBE6T-6 cells retaining two copies of chromosome 17. The loss occurred in PDL 50 in both UE6E7T-6 and UCB408E6E7TERT-33, and between PDL 78 and 101 in UE6E7T-3. Structural and numerical aberrations targeting chromosome 17 are often reported in tumors from various tissues (Olaharski et al. 2006), whereas the pattern that chromosome 13 is lost and chromosome 17 is stable, was common for the three cell lines in this study, indicating the possibility that the loss of chromosome 13 may play an important role in the chromosomal aberration of hMSCs to acquire growth advantages under the given culturing condition. Similar karyotypic changes were evident in cultured human embryonic stem cells, involving the gain of chromosome 17 or chromosome 12 (Carlson et al. 2000; Draper et al. 2004). It is thus conjectured that the aneuploidy developed through chromosomal loss from

diploid cells arises through different mechanisms from tetraploid intermediate.

An alternative explanation for aneuploid formation mechanism independent of tetraploid intermediate is loss of regulation in centrosome duplication, leading to abnormal centrosome amplification and multipolar spindles, resulting in aneuploidy. In addition, centrosome amplification caused by loss of p53 has been shown in cultured mouse cells (Fukasawa et al. 1996), but not in cultured human cells (Kawamura et al. 2004). However, loss of p53 and centrosome amplification has been revealed in human cancer tissue. Our preliminary examination has indicated a weak correlation between centrosome amplification and chromosome number (data not shown). Only 2.4% of UCBTERT-21 cells contained >3 centrosomes per cell, whereas 11.9% of UCB408E6E7TERT-33, 19.1% of UE6E7T-3 and 14.3% of UBE6T-6 cells contained >3 centrosomes per cell. Thus, further study is still needed to clarify the mechanism inducing chromosomal instability in immortalized hMSCs cultured over a long period.

Human mesenchymal stem cells are thought to be multipotent cells that can replicate stem cells and that can differentiate to lineages of mesenchymal tissues including bone, fat, tendon, and muscle. Our results indicated that immortalized hMSCs, except UCBTERT-21, induced changes in chromosome number over prolonged culture, but these cells have still retained the ability to both proliferate and differentiate. Immortalized UBE6T-6 cells also displayed neuron-like morphology and strong expression of the neuron-specific markers of neurofilament and III-β-tubulin. We previously demonstrated that hTERT, E7-immortalized hMSCs differentiate into neural cells in vitro on the basis of morphological changes, expression of neural markers such as nestin, neurofilament, MAP-2, Nurr1, and III-β-tubulin. Furthermore, the physiological function showed reversible calcium uptake in response to extracellular potassium concentration (Mori et al. 2005). Similar observations have been reported using rat MSCs (Wislet-Gendebien et al. 2003; Wislet-Gendebien et al. 2005; Pacary et al. 2006). In preliminary experiment of cell transplantation that 10^6 cells of UCBTERT-21 cell (PDLs 120) or UCB408E6E7TERT-33 cell (PDLs 200) were injected into nude mice subcutaneously, no tumorigenicity was observed (data not shown).

In conclusion, our study showed that the hTERT-immortalized cell line displayed normal karyotype and differentiation ability in prolonged culture. These results provide a step forward toward supplying a sufficient number of cells for new therapeutic approaches. In addition, oncogene-immortalized cell lines exhibited abnormal karyotype accompanying the preferential loss of chromosome 13 but without differential alteration during prolonged culture. Thus, the results could provide a useful model for understanding the mechanisms of the chromosomal instability and the differentiation of hMSC.

Acknowledgments This study was supported in part by a grant from the Ministry of Health, Labor and Welfare of Japan. We are grateful to Dr. T.Masui for his advice on ethics problems, and to Mr. H.Migitaka (Carl Zeiss Co., Ltd.) for his assistance with mFISH karyotype analysis. M.T. and K.T. contributed equally to this work.

References

Armanios, M.; Greider, C. W. Telomerase and cancer stem cells. Cold Spring Harbor Symp. Quant. Biol. 70:205–208; 2005.

Bodnar, A. G.; Ouellette, M.; Frolkis, M.; Holt, S. E.; Chiu, C. P.; Morin, G. B.; Harley, C. B.; Shay, J. W.; Lichtsteiner, S.; Wright, W. E. Extension of life-span by introduction of telomerase into normal human cells. Science 279:349–352; 1998.

Burns, J. S.; Abdallah, B. M.; Guldberg, P.; Rygaard, J.; Schroder, H. D.; Kassem, M. Tumorigenic heterogeneity in cancer stem cells evolved from long-term cultures of telomerase-immortalized human mesenchymal stem cells. Cancer Res. 65:3126–3135; 2005.

Carlson, J. A.; Healy, K.; Tran, T. A.; Malfetano, J.; Wilson, V. L.; Rohwedder, A.; Ross, J. S. Chromosome 17 aneusomy detected by fluorescence in situ hybridization in vulvar squamous cell carcinomas and synchronous vulvar skin. Am. J. Pathol. 157:973–983; 2000.

Chang, M. W.; Grillari, J.; Mayrhofer, C.; Fortschegger, K.; Allmaier, G.; Marzban, G.; Katinger, H.; Voglauer, R. Comparison of early passage, senescent and hTERT immortalized endothelial cells. Exp. Cell Res. 309:121–136; 2005.

Cross, S. M.; Sanchez, C. A.; Morgan, C. A.; Schimke, M. K.; Ramel, S.; Idzerda, R. L.; Raskind, W. H.; Reid, B. J. A p53-dependent mouse spindle checkpoint. Science 267:1353–1356; 1995.

Dickson, M. A.; Hahn, W. C.; Ino, Y.; Ronfard, V.; Wu, J. Y.; Weinberg, R. A.; Louis, D. N.; Li, F. P.; Rheinwald, J. G. Human keratinocytes that express hTERT and also bypass a p16(INK4a)-enforced mechanism that limits life span become immortal yet retain normal growth and differentiation characteristics. Mol. Cell Biol. 20:1436–1447; 2000.

Draper, J. S.; Smith, K.; Gokhale, P.; Moore, H. D.; Maltby, E.; Johnson, J.; Meisner, L.; Zwaka, T. P.; Thomson, J. A.; Andrews, P. W. Recurrent gain of chromosomes 17q and 12 in cultured human embryonic stem cells. Nat. Biotechnol. 22:53–54; 2004.

Duensing, S.; Lee, L. Y.; Duensing, A.; Basile, J.; Piboonniyom, S.; Gonzalez, S.; Crum, C. P.; Munger, K. The human papillomavirus type 16 E6 and E7 oncoproteins cooperate to induce mitotic defects and genomic instability by uncoupling centrosome duplication from the cell division cycle. Proc. Natl. Acad.Sci. U. S. A. 97:10002–10007; 2000.

Duensing, S.; Munger, K. The human papillomavirus type 16 E6 and E7 oncoproteins independently induce numerical and structural chromosome instability. Cancer Res. 62:7075–7082; 2002.

Fukasawa, K.; Choi, T.; Kuriyama, R.; Rulong, S.; Vande Woude, G. F. Abnormal centrosome amplification in the absence of p53. Science 271:1744–1747; 1996.

Harada, H.; Nakagawa, H.; Oyama, K.; Takaoka, M.; Andl, C. D.; Jacobmeier, B.; von, W. A.; Enders, G. H.; Opitz, O. G.; Rustgi, A. K. Telomerase induces immortalization of human esophageal keratinocytes without p16INK4a inactivation. Mol. Cancer Res. 1:729–738; 2003.

Kawamura, K.; Izumi, H.; Ma, Z.; Ikeda, R.; Moriyama, M.; Tanaka, T.; Nojima, T.; Levin, L. S.; Fujikawa-Yamamoto, K.; Suzuki, K.; Fukasawa, K. Induction of centrosome amplification and

chromosome instability in human bladder cancer cells by p53 mutation and cyclin E overexpression. Cancer Res. 64:4800–4809; 2004.

Khan, S. H.; Wahl, G. M. p53 and pRb prevent rereplication in response to microtubule inhibitors by mediating a reversible G1 arrest. Cancer Res. 58:396–401; 1998.

Kiyono, T.; Foster, S. A.; Koop, J. I.; McDougall, J. K.; Galloway, D. A.; Klingelhutz, A. J. Both Rb/p16INK4a inactivation and telomerase activity are required to immortalize human epithelial cells. Nature 396:84–88; 1998.

Makino, S.; Fukuda, K.; Miyoshi, S.; Konishi, F.; Kodama, H.; Pan, J.; Sano, M.; Takahashi, T.; Hori, S.; Abe, H.; Hata, J.; Umezawa, A.; Ogawa, S. Cardiomyocytes can be generated from marrow stromal cells in vitro. J. Clin. Invest. 103:697–705; 1999.

Milyavsky, M.; Shats, I.; Erez, N.; Tang, X.; Senderovich, S.; Meerson, A.; Tabach, Y.; Goldfinger, N.; Ginsberg, D.; Harris, C. C.; Rotter, V. Prolonged culture of telomerase-immortalized human fibroblasts leads to a premalignant phenotype. Cancer Res. 63:7147–7157; 2003.

Mori, T.; Kiyono, T.; Imabayashi, H.; Takeda, Y.; Tsuchiya, K.; Miyoshi, S.; Makino, H.; Matsumoto, K.; Saito, H.; Ogawa, S.; Sakamoto, M.; Hata, J.; Umezawa, A. Combination of hTERT and bmi-1, E6, or E7 induces prolongation of the life span of bone marrow stromal cells from an elderly donor without affecting their neurogenic potential. Mol. Cell Biol. 25:5183–5195; 2005.

Munger, K.; Baldwin, A.; Edwards, K. M.; Hayakawa, H.; Nguyen, C. L.; Owens, M.; Grace, M.; Huh, K. Mechanisms of human papillomavirus-induced oncogenesis. J. Virol. 78:11451–11460; 2004.

Munger, K.; Howley, P. M. Human papillomavirus immortalization and transformation functions. Virus Res. 89:213–228; 2002.

Okamoto, T.; Aoyama, T.; Nakayama, T.; Nakamata, T.; Hosaka, T.; Nishijo, K.; Nakamura, T.; Kiyono, T.; Toguchida, J. Clonal heterogeneity in differentiation potential of immortalized human mesenchymal stem cells3. Biochem. Biophys. Res. Commun. 295:354–361; 2002.

Olaharski, A. J.; Sotelo, R.; Solorza-Luna, G.; Gonsebatt, M. E.; Guzman, P.; Mohar, A.; Eastmond, D. A. Tetraploidy and chromosomal instability are early events during cervical carcinogenesis. Carcinogenesis 27:337–343; 2006.

Pacary, E.; Legros, H.; Valable, S.; Duchatelle, P.; Lecocq, M.; Petit, E.; Nicole, O.; Bernaudin, M. Synergistic effects of CoCl(2) and ROCK inhibition on mesenchymal stem cell differentiation into neuron-like cells. J. Cell Sci. 119:2667–2678; 2006.

Patel, D.; Incassati, A.; Wang, N.; McCance, D. J. Human papillomavirus type 16 E6 and E7 cause polyploidy in human keratinocytes and up-regulation of G2-M-phase proteins. Cancer Res. 64:1299–1306; 2004.

Pittenger, M. F.; Mackay, A. M.; Beck, S. C.; Jaiswal, R. K.; Douglas, R.; Mosca, J. D.; Moorman, M. A.; Simonetti, D. W.; Craig, S.; Marshak, D. R. Multilineage potential of adult human mesenchymal stem cells. Science 284:143–147; 1999.

Saito, M.; Handa, K.; Kiyono, T.; Hattori, S.; Yokoi, T.; Tsubakimoto, T.; Harada, H.; Noguchi, T.; Toyoda, M.; Sato, S.; Teranaka, T. Immortalization of cementoblast progenitor cells with Bmi-1 and TERT. J. Bone Miner. Res. 20:50–57; 2005.

Schaeffer, A. J.; Nguyen, M.; Liem, A.; Lee, D.; Montagna, C.; Lambert, P. F.; Ried, T.; Difilippantonio, M. J. E6 and E7 oncoproteins induce distinct patterns of chromosomal aneuploidy in skin tumors from transgenic mice. Cancer Res. 64:538–546; 2004.

Sen, S. Aneuploidy and cancer. Curr. Opin. Oncol. 12:82–88; 2000.

Shi, Q.; King, R. W. Chromosome nondisjunction yields tetraploid rather than aneuploid cells in human cell lines. Nature 437:1038–1042; 2005.

Solinas-Toldo, S.; Durst, M.; Lichter, P. Specific chromosomal imbalances in human papillomavirus-transfected cells during progression toward immortality. Proc. Natl. Acad. Sci. U. S. A 94:3854–3859; 1997.

Takeda, Y.; Mori, T.; Imabayashi, H.; Kiyono, T.; Gojo, S.; Miyoshi, S.; Hida, N.; Ita, M.; Segawa, K.; Ogawa, S.; Sakamoto, M.; Nakamura, S.; Umezawa, A. Can the life span of human marrow stromal cells be prolonged by bmi-1, E6, E7, and/or telomerase without affecting cardiomyogenic differentiation? J. Gene Med. 6:833–845; 2004.

Takeuchi, K.; Kuroda, K.; Ishigami, M.; Nakamura, T. Actin cytoskeleton of resting bovine platelets. Exp. Cell Res. 186:374–380; 1990.

Terai, M.; Uyama, T.; Sugiki, T.; Li, X. K.; Umezawa, A.; Kiyono, T. Immortalization of human fetal cells: the life span of umbilical cord blood-derived cells can be prolonged without manipulating p16INK4a/RB braking pathway. Mol. Biol. Cell 16:1491–1499; 2005.

Wislet-Gendebien, S.; Hans, G.; Leprince, P.; Rigo, J. M.; Moonen, G.; Rogister, B. Plasticity of cultured mesenchymal stem cells: switch from nestin-positive to excitable neuron-like phenotype. Stem Cells 23:392–402; 2005.

Wislet-Gendebien, S.; Leprince, P.; Moonen, G.; Rogister, B. Regulation of neural markers nestin and GFAP expression by cultivated bone marrow stromal cells. J. Cell Sci. 116:3295–3302; 2003.

Zheng, L.; Lee, W. H. The retinoblastoma gene: a prototypic and multifunctional tumor suppressor. Exp. Cell Res. 264:2–18; 2001.

Am J Physiol Gastrointest Liver Physiol 293: G1089–G1098, 2007.
First published September 20, 2007; doi:10.1152/ajpgi.00187.2007.

A role of Wnt/β-catenin signals in hepatic fate specification of human umbilical cord blood-derived mesenchymal stem cells

Yoko Yoshida,[1] Takashi Shimomura,[1] Tomohiko Sakabe,[1] Kyoko Ishii,[1] Kazue Gonda,[1] Saori Matsuoka,[1] Yumi Watanabe,[1] Kazuko Takubo,[2] Hiroyuki Tsuchiya,[1] Yoshiko Hoshikawa,[1] Akihiro Kurimasa,[1] Ichiro Hisatome,[3] Taro Uyama,[4] Masanori Terai,[4] Akihiro Umezawa,[4] and Goshi Shiota[1]

[1]*Division of Molecular and Genetic Medicine, Department of Genetic Medicine and Regenerative Therapeutics, Graduate School of Medicine, Tottori University;* [2]*Division of Oral and Maxillofacial Biopathological Surgery, Department of Medicine of Sensory and Motor Organs, Faculty of Medicine, Tottori University;* [3]*Division of Regenerative Medicine, Department of Genetic Medicine and Regenerative Therapeutics, Graduate School of Medicine, Tottori University; and* [4]*Department of Reproductive Biology and Pathology, National Research Institute for Child Health and Development, Tokyo, Japan*

Submitted 30 April 2007; accepted in final form 7 September 2007

Yoshida Y, Shimomura T, Sakabe T, Ishii K, Gonda K, Matsuoka S, Watanabe Y, Takubo K, Tsuchiya H, Hoshikawa Y, Kurimasa A, Hisatome I, Uyama T, Terai M, Umezawa A, Shiota G. A role of Wnt/β-catenin signals in hepatic fate specification of human umbilical cord blood-derived mesenchymal stem cells. *Am J Physiol Gastrointest Liver Physiol* 293: G1089–G1098, 2007. First published September 20, 2007; doi:10.1152/ajpgi.00187.2007.—Human umbilical cord blood-derived mesenchymal stem cells (UCBMSCs) are expected to be an excellent source of cells for transplantation. In addition, the stem cell plasticity of human UCBMSCs, which can transdifferentiate into hepatocytes, has been reported. However, the mechanisms involved remain to be clarified. To identify the genes and/or signals that are important in specifying the hepatic fate of human UCBMSCs, we analyzed gene expression profiles during the hepatic differentiation of UCBMSCs with human telomerase reverse transcriptase, UCBMSCs immortalized by infection with a retrovirus carrying telomerase reverse transcriptase, but whose differentiation potential remains unchanged. Efficient differentiation was induced by 5-azacytidine (5-aza)/hepatocyte growth factor (HGF)/oncostatin M (OSM)/fibroblast growth factor 2 (FGF2) treatment in terms of function as well as protein expression: 2.5-fold increase in albumin, 4-fold increase in CCAAT enhancer-binding protein α, 1.5-fold increase in cytochrome p450 1A1/2, and 8-fold increase in periodic acid-Schiff staining. Consequently, we found that the expression of Wnt/β-catenin-related genes downregulated, and the translocation of β-catenin was observed along the cell membrane and in the cytoplasm, although some β-catenin was still in the nucleus. Downregulation of Wnt/β-catenin signals in the cells by Fz8-small interference RNA treatment, which was analyzed with a Tcf4 promoter-luciferase assay, resulted in similar hepatic differentiation to that observed with 5-azacytidine/HGF/OSM/FGF2. In addition, the subcellular distribution of β-catenin was similar to that of cells treated with 5-azacytidine/HGF/OSM/FGF2. In conclusion, the suppression of Wnt/β-catenin signaling induced the hepatic differentiation of UCBMSCs, suggesting that Wnt/β-catenin signals play an important role in the hepatic fate specification of human UCBMSCs.

mesenchymal stem cell; Wnt/β-catenin signaling pathway; hepatic differentiation

HUMAN UMBILICAL CORD BLOOD (UCB) has been reported to contain stem/progenitor cells at concentrations greater than or equal to those in bone marrow and adult peripheral blood (28, 30). In addition, the use of UCB entails few ethical problems, and even now most UCB is regarded as medical waste in delivery rooms. Although bone marrow is an important source of stem cells, its use has several disadvantages: aspirating bone marrow from patients is an invasive procedure, and the capacity of stem cells to differentiate decreases with the donor's age (7). UCB-cell transplantation for various blood diseases has recently been successful, with a lower incidence of graft-vs.-host disease than that seen in many conventional treatments (18). Thus UCB is considered useful for therapeutic applications.

It has long been thought that the differentiation potential of adult stem cells is limited to their germ layer of origin, but recent studies have demonstrated that adult stem cells are more plastic than once believed (1, 20–22, 47). Mesenchymal stem cells (MSCs) can differentiate into several lineages including osteoblasts, chondrocytes, and adipocytes. Recently, in vivo transplantation studies showed that MSCs can differentiate into endodermal cell types as well as most mesodermal and neuroectodermal types (15). Human MSCs from bone marrow and UCB-derived MSCs (UCBMSCs) can differentiate into hepatocytes in vitro (41, 24, 25). UCBMSC may become an important alternative source of cells for transplantation; however, the hepatic differentiation of MSCs is not efficient enough for clinical use. Therefore, the molecular mechanism of hepatic differentiation should be clarified. Newly established UCBMSCs with human telomerase reverse transcriptase (UCBTERT) proliferated for >120 population doublings, and the characteristics of the cells including differentiation potential remained unchanged (46). Therefore, UCBTERT cells provide a powerful model for the application of stem cell-based therapies.

Adult stem cells, under certain microenvironmental conditions, give rise to cell types besides the cell type of origin, indicating that they can switch cell fate, a feature termed "stem cell plasticity" (23). An alternative mechanism to induce cell plasticity could be the cell fusion of a bone marrow-derived cell with a nonhematopoietic cell (19). Although use of the Cre/loxP system revealed that some hepatocytes from bone marrow-derived cells are really produced by cell fusion in vivo (2), in vitro hepatic differentiation of MSCs demonstrated that

Address for reprint requests and other correspondence: G. Shiota, Division of Molecular and Genetic Medicine, Dept. of Genetic Medicine and Regenerative Therapeutics, Graduate School of Medicine, Tottori Univ., Yonago 683-8504, Japan (e-mail: gshiota@grape.med.tottori-u.ac.jp).

The costs of publication of this article were defrayed in part by the payment of page charges. The article must therefore be hereby marked "*advertisement*" in accordance with 18 U.S.C. Section 1734 solely to indicate this fact.

stem cell plasticity really exists (24, 25). In addition, we previously reported that the hepatic differentiation of UCB cells as well as cell fusion occurred simultaneously in vivo (45). Since cells generated from cell fusions may be more likely to undergo transformation, hepatocytes differentiated from UCB cells in vitro, which do not mediate cell fusion, are a reliable cell source for regenerative medicine. We therefore attempted to identify the genes and/or signals that regulate the hepatic differentiation of human UCBMSCs.

MATERIALS AND METHODS

Materials. Fibroblast growth factor 2 (FGF2), hepatocyte growth factor (HGF), and oncostatin M (OSM) were purchased from PeproTech EC (London, UK). Recombinant Wnt-3A was obtained from R&D Systems. Mesenchymal stem cell growth medium (MSCGM, PT-3001) and SYTOX green nucleic acid stain were purchased from Cambrex Bio Science. 5-Azacytidine (5-aza) was obtained from Nacalai Tesque (Kyoto, Japan). Anti-human serum albumin antibody (A 6684), anti-C/EBPα antibody (sc-61), and anti-CYP1A1/1A2 (AB1255), and Cy3-conjugated secondary antibody (AP132C) were purchased from Sigma Aldrich (St. Louis, MO), Santa Cruz Biotechnology (Santa Cruz, CA), and Chemicon International, respectively.

Culture of UCBTERT-21 cells. Human UCBMSCs, the life span of which was prolonged by infection with a retrovirus encoding human telomerase reverse transcriptase (hTERT), designated UCBTERT-21 cells (46), were used. All cultures were maintained at 37°C in a humidified atmosphere containing 95% air and 5% CO_2. To induce the hepatic differentiation of UCBTERT-21 cells in vitro, we added several cytokines to the culture media. UCBTERT-21 cells were plated into six-well plates at 2×10^4 cells/well and cultured overnight to allow cell attachment. To induce hepatic differentiation, UCBTERT-21 cells were cultured in MSCGM containing 1 μM 5-aza for 24 h and then cultured in MSCGM containing 10% FBS, 10 ng/ml FGF2, 20 ng/ml HGF, and 20 ng/ml OSM for 3 wk with special reference to Refs. 25, 29, and 41. The medium was changed weekly (Fig. 1). Hepatic differentiation was assessed by reverse transcription-polymerase chain reaction (RT-PCR), immunostaining, periodic acid-Schiff (PAS) staining, and urea assay.

RNA extraction and RT-PCR analysis. Total RNA was extracted from UCBTERT-21 cells by using a Total RNA Isolation kit (Promega, Madison, WI). cDNA samples were synthesized from 1 μg of total RNA by using a Super Script II first-strand synthesis system (Invitrogen, Carlsbad, CA) with a-oligo(dT)-adaptor primer according to the manufacturer's instructions. The cDNA preparation template was used for subsequent PCR amplification by using *Taq* DNA polymerase. The primers for albumin, CCAAT/enhancer-binding protein α (C/EBPα), CCAAT/enhancer-binding protein β (C/EBPβ), cytochrome p4501A1 (CYP1A1), cytochrome p4501A2 (CYP1A2), phosphoenolpyruvate carboxykinase (PEPCK), and GAPDH were as follows: albumin forward primer, 5′-TTGGAAAAATCCCACTGCAT-3′; albumin reverse primer, 5′-CTCCAAGCTGCTCAAAAAGC-3′; C/EBPα forward primer, 5′-CACGAAGCACGATCAGTCCAT-3′; C/EBPα reverse primer, 5′-CGCACATTCACATTGCACAAG-3′; C/EBPβ forward primer, 5′-GCCAAGAAGACCGTGGACA-3′; C/EBPβ reverse primer, 5′-GCCAAGAAGACCGTGGACA-3′; CYP1A1 forward primer, 5′-ACCATGACCAGAAGCTATGGGT-3′; CYP1A1 reverse primer, 5′-TTAACACCTTGTCGATAGCACCA-3′; CYP1A2 forward primer, 5′-ACCATGACCCAGAGCTGTGG-3′; CYP1A2 reverse primer, 5′-TCACTCAAGGGCTTGTTAAT-3′ PEPCK forward primer, 5′-CAGGCAGCTGAAGAAGTATGA-3′, PEPCK reverse primer, 5′-AACCGTCTTGCTTTCGATCCT-3′, GAPDH forward primer, 5′-GTCTTCTCCACCATGGAGAAGGCT-3′; GAPDH reverse primer, 5′-CATGCCAGTGAGCTTCCCGTTCA-3′. Albumin was amplified at 95°C for 2 min, with denaturing at 95°C for 30 s, annealing at 58°C for 30 s, and extension at 72°C for 30 s for 35 cycles. GAPDH was amplified at 95°C for 2 min, with denaturing at 95°C 30 s, annealing at 60°C for 30 s, and extension at 72°C for 30 s for 30 cycles. The PCR products were analyzed by electrophoresis with a 2% agarose gel and stained with ethidium bromide. The intensity of the UV-light illuminated bands was measured by ImageJ (http://rsb.info.nih.gov/ij/) and was expressed after being normalized to GAPDH. Control RNA from normal adult liver was obtained when a patient with colon cancer metastasis underwent partial hepatectomy under informed consent.

Real-time quantitative PCR analysis. The cDNA template was amplified by use of a LightCycler (Roche). β-Actin was employed as an internal reference gene to normalize cDNA input. The mRNA expression levels of β-catenin, PP2A, and frizzled 8 (Fz8) were defined as the ratio of the value of each gene product to that of the β-actin product. The primers were as follows: albumin forward primer, 5′- TGTTGCATGAGAAAACGCCA-3′; albumin reverse primer, 5′- GTCGCCTGTTCACCAAGGAT-3′; Fz8 forward primer, 5′-TCTGGTGGGTGATCTTGTCG-3′; Fz8 reverse primer, 5′-AGCACCGCGATGGACTTGAC-3′; β-actin forward primer, 5′-CACTCTTCCAGCCTTCCTTCC-3′; β-actin reverse primer, 5′-CGTACAGGTCTTTGCGGATGTC-3′. The real-time PCR assays were performed with SYBR green (Roche) according to the manufacturer's instructions.

PAS staining for glycogen. Cells were fixed with PBS containing 4% formaldehyde for 20 min, permeabilized with PBS containing 0.1% Triton X-100 for 10 min, and incubated in the presence or absence of 1 mg/ml diastase for 1 h at 37°C. Samples were then oxidized in 1% periodic acid for 5 min, treated with Schiff's reagent for 15 min, rinsed three times in a sodium sulfite solution (0.5% sodium sulfite, 0.05 N HCl), and rinsed another three times in H_2O. Sections were assessed under a light microscope.

Urea assay. UCBTERT-21 cells at 1×10^5 cells/well were cultured, and the cell density was adjusted weekly. After 3 wk, 3×10^4 cells were incubated with 5 mM ammonium chloride, and the amount of urea secreted into the medium was measured every 24 h for up to 96 h. Urea concentrations were determined with a QuantiChrom urea assay kit (BioAssay Systems) according to the manufacturer's instructions.

Immunocytochemistry. Cultures were collected by enzymatic methods and were plated onto coverslips. The coverslips were fixed in PBS containing 4% formaldehyde for 20 min and permeabilized with PBS containing 0.2% Triton X-100 for 10 min. Samples were blocked with goat serum for 20 min and then incubated with anti-human serum albumin, anti-human C/EBPα, anti-CYP1A1/1A2, or anti-β-catenin antibodies, followed by Vectastain ABC Systems (Vector Laboratories, Burlingame, CA) or Cy3-conjugated secondary antibody. Hematoxylin or SYTOX green was utilized for nuclear counterstaining. The

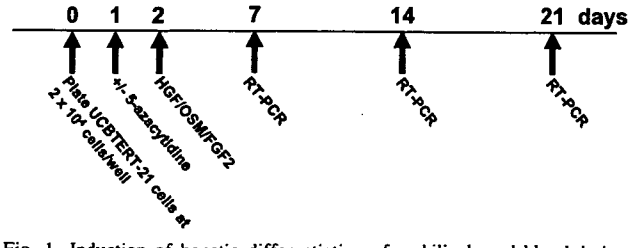

Fig. 1. Induction of hepatic differentiation of umbilical cord blood-derived mesenchymal stem cells with human telomerase reverse transcriptase (UCBTERT-21) cells. Experimental protocol. UCBTERT-21 cells were transferred into 6-well plates at 2×10^4 cells/well. The cells were cultured in mesenchymal stem cell growth medium (MSCGM) with or without 1 μM 5-azacytidine (5-aza) or not for 24 h and then cultured in MSCGM containing 20 ng/ml hepatocyte growth factor (HGF), 20 ng/ml oncostatin M (OSM), and/or 10 ng/ml fibroblast growth factor 2 (FGF2) for 3 wk. The culture medium was exchanged weekly. Total RNA was extracted from the UCBTERT-21 cells for RT-PCR.

coverslips were mounted with Gel/Mount, and the sections were assessed under a light microscope or fluorescence microscope.

DNA microarrays. RNA was extracted from UCBTERT-21 cells treated with or without 5-aza/HGF/OSM/FGF2 on *day 7* by use of an RNeasy mini kit (Qiagen), followed by digestion with RNase-free DNase (Qiagen). DNA microarray analysis was performed using AceGene human oligo chip 30k 1 chip version (Hitachi Software Engineering, Yokohama, Japan), which contains the oligonucleotide probe sets for 30,000 human genes. The intensity of fluorescence of each probe was measured with a Fuji FLA-8000 scanner (FujiPhoto Film, Tokyo, Japan) and quantified using Array Gauge software (FujiPhoto Film). The expression of each gene was compared between UCBTERT-21 cells treated with and without 5-aza/HGF/OSM/FGF2.

Transfection of siRNA. The Fz8 small interference RNA (siRNA; Fzd8-siRNA, cat. SI02646413) and nonsilencing siRNA control (negative control siRNA, cat. 1022563) were purchased from Qiagen. UCBTERT-21 cells were transfected with siRNA in multiwell plates by using RNAiFect transfection reagent (Qiagen). A mixture of 1 μg siRNA, 100 μl Buffer EC-R, and 6 μl RNAiFect transfection reagent was incubated for 15 min at room temperature. One hundred microliters of the mixture and 300 μl of medium containing 10% FBS were incubated with the cells for 6 h. The effect of mRNA silencing was confirmed by real-time quantitative PCR analysis.

Gene reporter assay. The plasmid Tcf4-CMVpro-Luc contains three copies of the optimal Tcf motif CCTTTGATC upstream of the CMV promoter that drives the expression of luciferase (Fig. 4*B*) (38). The CMV promoter sequence was inserted into pGL3-Basic vector (Promega). The plasmid pRL-TK (Promega) was used as an internal control. Transient transfection was performed using RNAiFect transfection reagent. As a positive control, 100 ng/ml of Wnt-3a was added 24 h after transfection. At 48 h after transfection, the cell lysates were used for gene reporter assays with the Dual-Luciferase reporter assay system (Promega).

RESULTS

Optimal conditions for hepatic differentiation. UCBTERT-21 cells are suitable for this study because they proliferate clonally and expand for a prolonged number of passages, and, importantly, introduction of the hTERT gene did not change the characteristics of the cells (46). UCBTERT-21 cells were expanded in six-well plates at 2.0×10^4 cells/well. The cells were cultured first with or without 5-aza for 24 h and then with a combination of HGF, OSM, and FGF2 for 3 wk (Fig. 1). Albumin mRNA expression was evaluated by RT-PCR with seven combinations of these agents: 5-aza/HGF/OSM/FGF2, 5-aza/HGF/OSM, 5-aza/HGF, 5-aza, HGF/OSM/FGF2, HGF/OSM, and HGF compared with 10% FBS. On *day 0*, UCBTERT-21 cells expressed little albumin mRNA, and MSCGH scarcely expressed albumin mRNA without 5-aza or cytokines. The combination of 5-aza/HGF/OSM/FGF2 for 3 wk was more effective than the other seven combinations (data not shown).

To more precisely examine albumin mRNA expression, real-time PCR was performed using RNA obtained under optimal conditions and from the controls (Fig. 2*A*). The expression level of albumin mRNA after treatment with 5-aza/HGF/OSM/FGF2 was almost eightfold higher than that in MSCGM containing 10% FBS. We investigated whether UCBTERT-21 cells subjected to theses conditions expressed hepatocyte-specific proteins by immunocytochemistry. The expression of albumin was upregulated in the cells treated with 5-aza/HGF/OSM/FGF2, especially in the cells that proliferated at high density (Fig. 2*B*, *a* and *e*). Staining of C/EBPα was also increased, and the nuclei of treated cells were stained strongly (Fig. 2*B*, *b* and *f*). CYP1A1/2 staining was weak in untreated cells, but it was more intense in treated cells (Fig. 2*B*, *c* and *g*). The cells positive for CYP1A/2 were larger than those negative for CYP1A/2. The presence of stored glycogen, as determined by PAS staining, was observed in treated cells (Fig. 2*B*, *d* and *h*). Untreated cells did not show the ability to synthesize glycogen. When pretreated with diastase to digest glycogen, treated cells stained negative for glycogen (data not shown).

The level of cells positive for hepatic marker proteins and PAS staining in UCBTERT-21 cells treated with 5-aza/HGF/OSM/FGF2 significantly increased, compared with the control: a 2.5-fold increase in albumin, 4-fold increase in C/EBPα, 1.5-fold increase in CYP1A1/1A2, and 8-fold increase in PAS staining were induced by this treatment ($P < 0.01$, $P < 0.01$, $P < 0.05$, and $P < 0.01$, respectively, Fig. 2*C*).

Secretion of urea by the cells was measured every 24 h after the addition of 5 mM ammonium chloride. Urea in the medium became detectable at 24 h in both treated and untreated cells and increased thereafter, tending to be higher in the treated cells at 48 and 72 h. At 96 h, the production of urea was significantly greater in the treated cells compared with the control ($P < 0.05$, Fig. 2*D*).

The expression levels of albumin, C/EBPα, c/EBPβ, CYP1A1, Cyp1A2, and PEPCK were examined by RT-PCR (Fig. 2*E*). The expression levels of albumin, C/EBPα, C/EBPβ, CYP1A1, CYP1A2, and PEPCK were strongly induced in UCBTERT cells treated with 5-aza/HGF/OSM/FGF2. However, the expression levels of albumin, C/EBPα, C/EBPβ, CYP1A1, CYP1A2, and PEPCK in adult normal liver cells were 1.7-fold, 2.0-fold, 1.1-fold, 0.7-fold, and 3.5-fold greater than that of the treatment with 5-aza/HGF/OSM/FGF2. These findings suggest that UCBTERT cells treated with 5-aza/HGF/OSM/FGF2 were still immature compared with adult mature hepatocytes.

Genes that are associated with hepatic differentiation of human MSCs. We investigated the genes whose expression changed during the treatment with 5-aza/HGF/OSM/FGF2. Total RNA extracted from cells, that were treated with 5-aza/HGF/OSM/FGF2 or control medium for one wk, was examined by microarray analysis. We found that the expression levels of many Wnt signal-related molecules were downregulated in the treated cells, compared with the untreated cells (Table 1). The expression level of CTNNB1 (β-catenin) and many of the Fz family genes was decreased, including the expression level of Fz8. On the other hand, the expression level of CTNNBIP1 (ICAT), which inhibits Wnt signaling (44), increased by 2.4-fold. The expression of PPP2CA (protein phosphatase 2 catalytic subunit), which has a positive role in Wnt signal transduction (36), decreased. Conversely, the expression level of PPP2R1B (protein phosphatase regulatory subunit), which inhibits Wnt signaling (27), increased. Real-time RT-PCR analysis showed that β-catenin, PPA2CA, and Fz8 were downregulated in their expression (Fig. 3*A*); treatment with 5-aza/HGF/OSM/FGF2 reduced the expression of β-catenin, PPA2CA, and Fz8 to 82, 78, and 25%, respectively, of the control. Fz8 maintained its expression at ~20–40% of the control level during the course of hepatic differentiation of UCBMSC (Fig. 3*B*).

Subcellular distribution of β-catenin during hepatic localization. We investigated the subcellular localization of β-catenin in UCBTERT-21 cells by immunocytochemistry. β-Cate-

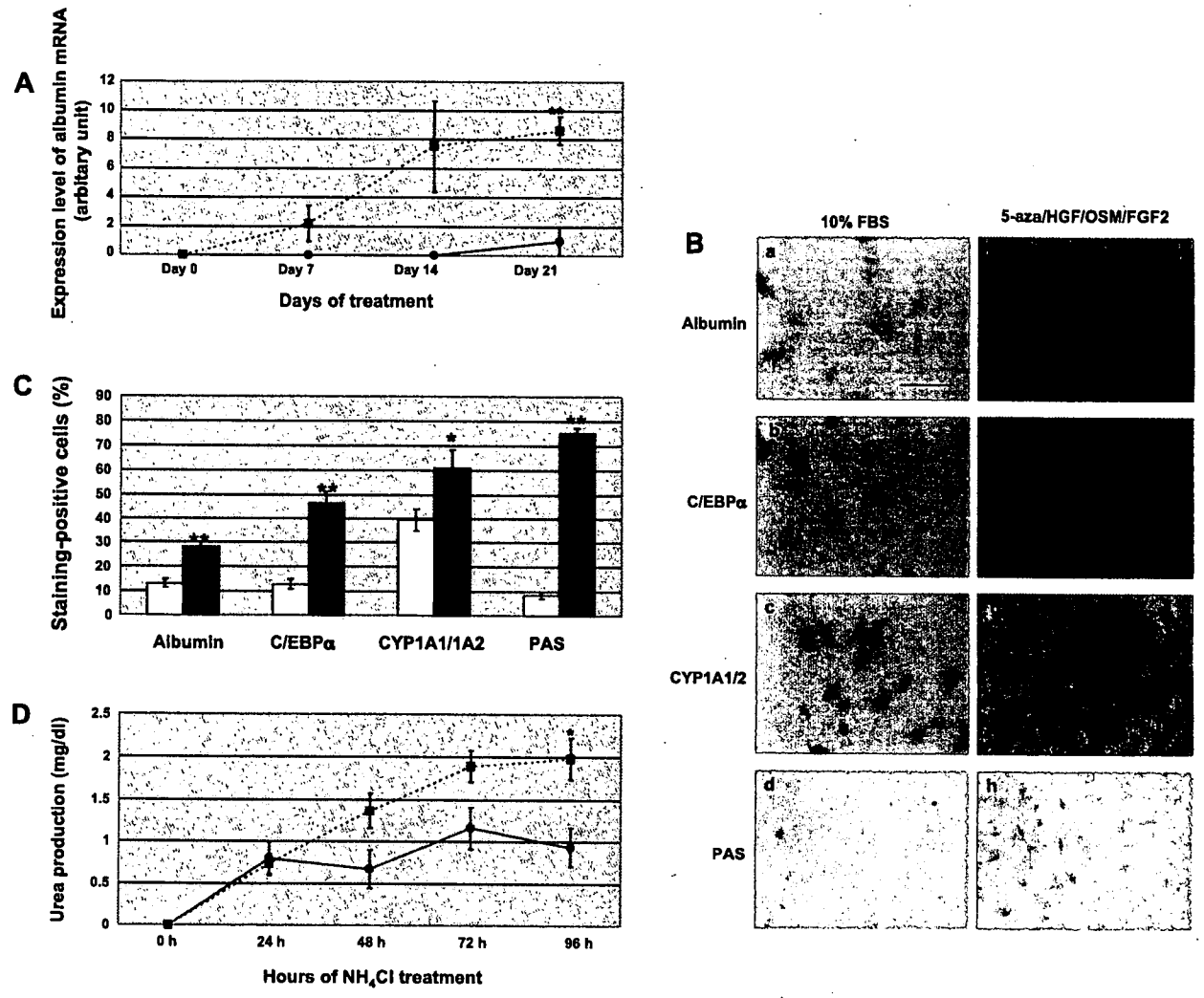

Fig. 2. Hepatic differentiation of UCBTERT-21 cells. *A*: expression of the albumin gene evaluated by quantitative real-time RT-PCR. The level of albumin gene expression is shown as a ratio of that in the control on *day 21*. ●, 10% FBS (control); ■, 10% FBS with 5-aza/HGF/OSM/FGF2. Data are expressed as means ± SE of 3 experiments. $^{**}P < 0.01$ compared with the control. *B*: induction of hepatic specific genes in UCBTERT-21 cells on *day 21* was analyzed by cytochemistry. *a–d*, 10% FBS; *e–h*, 10% FBS with 5-aza/HGF/OSM/FGF2. Cells were immunostained with anti-albumin (*a*, *e*), anti-CCAAT enhancer-binding protein α (C/EBPα) (*b*, *f*), and anti-cytochrome p450 1A1/2 (CYP1A1/1A2) (*c*, *g*) antibodies. Glycogen stored in the cells was stained by periodic acid-Schiff (PAS) stain (*d*, *h*). Scale bar, 100 μm. *C*: efficiency of hepatic differentiation of UCBTERT-21 cells on *day 21*. Open bars, 10% FBS (control); solid bars, 10% FBS with 5-aza/HGF/OSM/FGF2. Data are expressed as means ± SE of 6 experiments. $^{**}P < 0.01$, $^{*}P < 0.05$, compared with control. *D*: urea production in the culture medium of differentiated UCBTERT-21 cells. ●, 10% FBS (control); ■, 10% FBS with 5-aza/HGF/OSM/FGF2. Data are expressed as means ± SE of 6 experiments. $^{*}P < 0.05$, compared with control. *Fig. 2 (Continues).*

nin has dual roles, as an adhesion molecule at the plasma membrane and as a key intermediate in the canonical Wnt signaling pathway. On activation of the Wnt cascade, β-catenin in the cytosolic soluble pool becomes stabilized and then translocates into the nucleus where it coactivates transcription factors of the TCF/LEF family (4). On *day 7* after the start of treatment, β-catenin was mostly located in the nuclei of the cells (Fig. 3*C*). On *day 14* and *day 21*, β-catenin was also observed along the cell membrane and in the cytoplasm, but some was still in the nucleus (Fig. 3*C*). The translocation of β-catenin was observed during hepatic cell differentiation (5, 31). Thus the changes in β-catenin localization may be important during hepatic differentiation of progenitor cells.

Knockdown of the genes of MSC leading to hepatic differentiation. Since the expression levels of β-catenin, PP2CA, and Fz8 were downregulated during the course of hepatic differentiation of UCBTERT-21 cells, the suppressive effect of Fz8, which is essential for Wnt/β-catenin signaling (4), on hepatic differentiation was examined by using RNA interference. First, we confirmed that the expression level of Fz8 mRNA in Fz8-siRNA-transfected cells was decreased to 60% of that at 0 h at 48 h after transfection (Fig. 4*A*). To investigate the effect of Fz8 knockdown on β-catenin/TCF4 transcriptional activity, we performed a luciferase reporter assay with pTcf4-CMVpro-Luc, using pRL-TK as an internal control (Fig. 4*B*). Treatment with Wnt-3a enhanced luciferase activity,

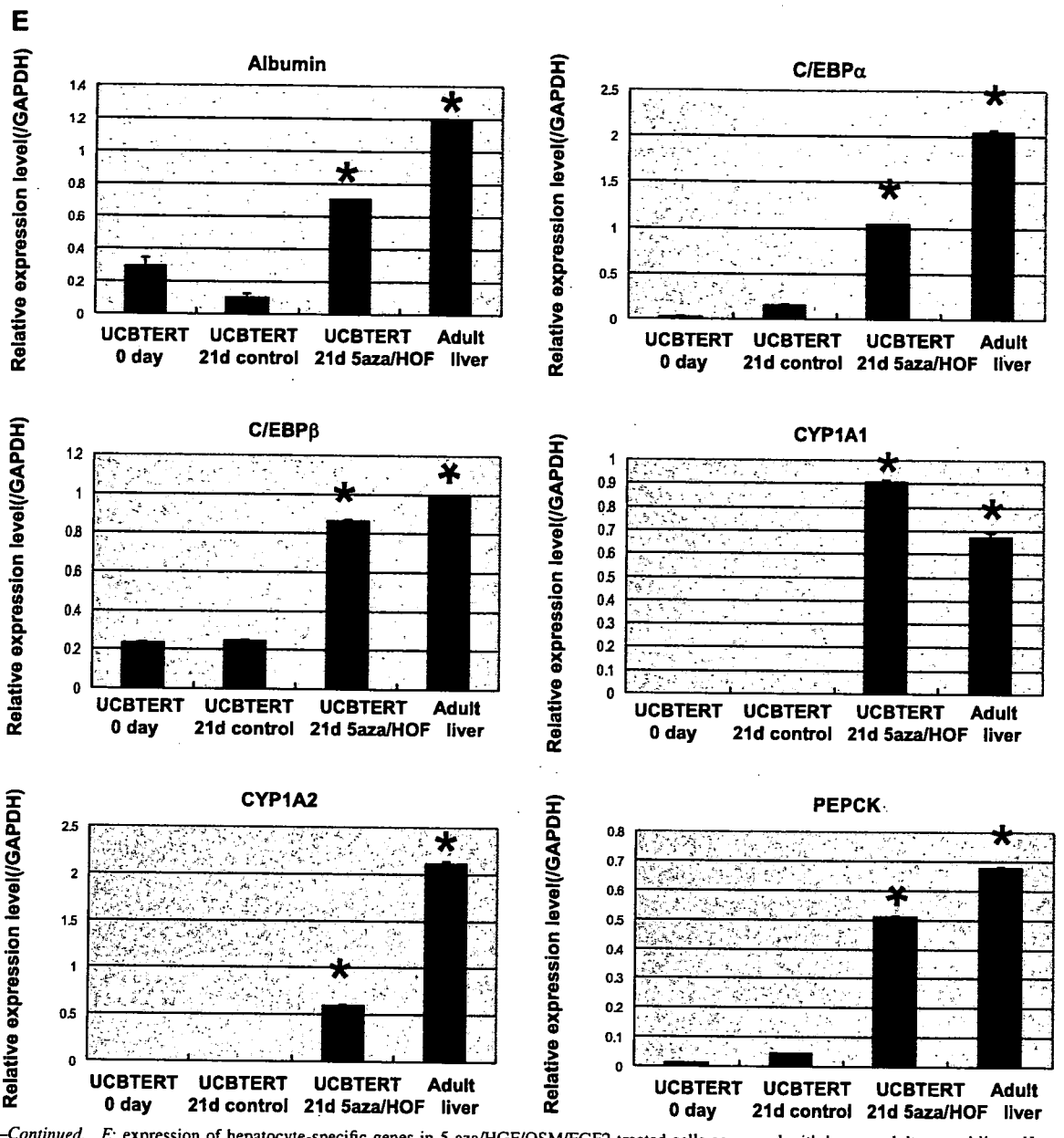

Fig. 2—*Continued.* *E*: expression of hepatocyte-specific genes in 5-aza/HGF/OSM/FGF2-treated cells compared with human adult normal liver. Hepatocyte-specific genes included albumin, C/EBPα, C/EBPβ, CYP1A1, CYP1A2, and phosphoenolpyruvate carboxykinase (PEPCK). PEPCK is the rate-limiting enzyme of glucogenesis. UCBTERT *day 0*, UCBTERT 21d control, UCBTERT 21d 5-aza/HOF, and Adult liver represent UCBTERT cells before incubation, cells incubated in 10% FBS for 21 days, cells incubated in 5-aza/HGF/OSM/FGF2 for 21 days, and adult liver tissue, respectively. Data are expressed as means ± SE of 3 experiments. $*P < 0.05$, compared with UCBTERT *day 0*.

whereas the luciferase activity in the cells transfected with Fz8-siRNA was 25% of that in the cells transfected with control siRNA, indicating that Wnt/β-catenin signaling was suppressed by transfection with Fz8-siRNA (Fig. 4*C*). Because the suppressive effect of transfection with lipofection reagent did not last more than 7 days (data not shown), transfection with Fz8-siRNA was repeated every 7 days. Weekly transfection of Fz8-siRNA caused an increase in albumin mRNA expression in UCBTERT-21 cells on *day 14* and *day 21*, as observed in UCBTERT-21 cells treated with 5-aza and cytokines (Fig. 4*D*).

UCBTERT-21 cells 3 wk after the beginning of Fz8-siRNA treatment were examined for hepatic marker proteins. Suppression of Fz8 by siRNA transfection induced the expression of albumin, C/EBPα, and CYP1A1/2 in UCBTERT-21 cells (Fig. 4*E*). The UCBTERT-21 cells treated with Fz8-siRNA were rounder than those subjected to "hepatic induction treatment." The numbers of albumin-, C/EBPα-, CYP1A1/2-, and PAS-

Table 1. *Microarray analysis of Wnt signal-related genes*

Name	Description	Accession Number	Ratio
CTNNB1	catenin (cadherin-associated protein), beta 1 (88kd); ctnnb1	NM_001904	0.409285785
CTNNBIP1	beta-catenin-interacting protein icat; ctnnbip1	NM_020248	2.445343626
FZ1	frizzled 1; fzd1	NM_003505	0.664559843
FZ2	frizzled-2; fzd2	AB017364	1.302192999
FZ3	frizzled homolog 3; fzd3	AJ272427	0
FZ3	frizzled homolog 3 (*Drosophila*); fzd3	NM_017412	0
FZ4	frizzled homolog 4 (*Drosophila*); fzd4	NM_012193	0.815346448
FZ5	frizzled 5; fzd5	NM_003468	0
FZ6	frizzled 6; fzd6	NM_003506	0
FZ7	frizzled 7; fzd7	NM_003507	0.800848224
FZ8	seven-transmembrane receptor frizzled-8; fzd8	AB043703	0.479522821
FZ9	frizzled 9; fzd9	NM_003508	0
FZ10	frizzled homolog 10 (*Drosophila*); fzd10	NM_007197	0.662549833
PPP2CA	protein phosphatase 2 (formerly 2a), catalytic subunit, alpha isoform; ppp2ca	NM_002715	0.177625911
PPP2CB	protein phosphatase 2 (formerly 2a), catalytic subunit, beta isoform; ppp2cb	NM_004156	0.642124376
PPP2R1A	protein phosphatase 2 (formerly 2a), regulatory subunit a (pr 65), alpha isoform; ppp2r1a	NM_014225	0.89013334
PPP2R1B	protein phosphatase 2 (formerly 2a), regulatory subunit a (pr 65), beta isoform; ppp2r1b	NM_002716	2.005757068
SFRP1	secreted apoptosis related protein 2; sarp2	AF017987	0.849458445
SFRP2	similar to stromal cell derived factor 5	BC008666	0
SFRP4	secreted frizzled-related protein 4; sfrp4	NM_003014	1.937534515
WNT1	wingless-type mmtv integration site family, member 1 precursor; wnt1	NM_005430	0
WNT2	ensemble prediction	ENSG00000105989	0.96735482
WNT2B	wingless-type mmtv integration site family, member 2b, isoform wnt-2b1; wnt2b	NM_004185	0
WNT2B	wingless-type mmtv integration site family, member 2b, isoform wnt-2b2; wnt2b	NM_024494	0
WNT4	wnt4 precursor; wnt4	AY009398	0.900795213
WNT5A	wingless-type mmtv integration site family, member 5a precursor; wnt5a	NM_003392	0
WNT6	similar to wingless-related mmtv integration site 6	BC004329	0
WNT7A	wingless-type mmtv integration site family, member 7a precursor; wnt7a	NM_004625	0
WNT8B	wingless-type mmtv integration site family, member 8b precursor; wnt8b	NM_003393	1.052495538
WNT9A	wnt14	AB060283	0.47555091
WNT9B	wnt-like protein wnt15; wnt15	AF028703	0
WNT10A	wingless-type mmtv integration site family, member 10a precursor; wnt10a	NM_025216	0
WNT10B	wingless-type mmtv integration site family, member 10b precursor; wnt10b	NM_003394	1.247761639
WNT11	wingless-type mmtv integration site family, member 11 precursor; wnt11	NM_004626	0
WNT16	wingless-type mmtv integration site family, member 16, isoform 2; wnt16	NM_016087	0.911155662

positive cells increased by 3.2-fold, 3-fold, 1.7-fold, and 6-fold, respectively (each, $P < 0.01$, Fig. 4*F*). However, there was no significant change in urea synthesis when the cells were transfected with Fd8-siRNA (data not shown).

The subcellular distribution of β-catenin in UCBTERT-21 cells transfected with Fz8-siRNA was investigated by immunocytochemistry. β-Catenin was located along the cell membrane and in the cytoplasm of the cells transfected with Fz8-siRNA (Fig. 4*G*).

DISCUSSION

In the present study, we identified an important signal for hepatic fate specification by using a system to induce hepatocytes to differentiate from human UCBMSCs. The combination of HGF, OSM, and FGF2 was examined, since the receptors for these cytokines were highly expressed on UCBTERT-21 cells (data not shown). In addition, during embryonic development, the production of growth factors such as HGF and FGFs has been associated with endoderm specification (40, 16). Furthermore, the first event that occurs after acute hepatitis in humans is a large increase in the serum level of HGF (42), suggesting that HGF plays an important role in the early stages of hepatogenesis. 5-Aza was employed because its efficiency in terms of cardiomyogenic differentiation of murine bone marrow stromal cells was ~30% (29). There is now evidence that the remodeling of chromatin and the alterations of epigenetics, including histone methylation and acetylation and DNA methylation, can cause committed cells to convert from one fate to another (6, 19). In our preliminary experiment, trichostatin A, a histone deacetylase inhibitor, induced apoptosis, but not differentiation, of UCBTERT-21 cells. Hence trichostatin A was not used in the present study. The positive rates of albumin, C/EBPα, CYP1A1/2, and PAS staining were not identical. This phenomenon may be explained by differences in the sensitivity of the immunostaining. In addition, the hierarchy of expression of liver-enriched transcription factors and proteins during development may explain this discrepancy (48).

Human UCBMSCs are easy to isolate but difficult to study because of their limited life span. The advantages of using UCBTERT-21 cells in a repopulation study are as follows: the cells have the same expression pattern of surface markers as the parental cells, the cells displayed osteogenic and adipogenic differentiation, the cells do not transform, they do not generate tumors in immunosuppressed mice, they do not form foci in vitro, and they stop dividing when confluent (46). Although important concerns regarding the use of these "artificial" cells, into which the hTERT genes has been introduced, for human liver repopulation studies may be raised, the use of UCBTERT-21 cells meets the purpose of the present study. In addition, the use of these cells enabled us to demonstrate the reversibility of differentiation. Therefore, to establish an effi-

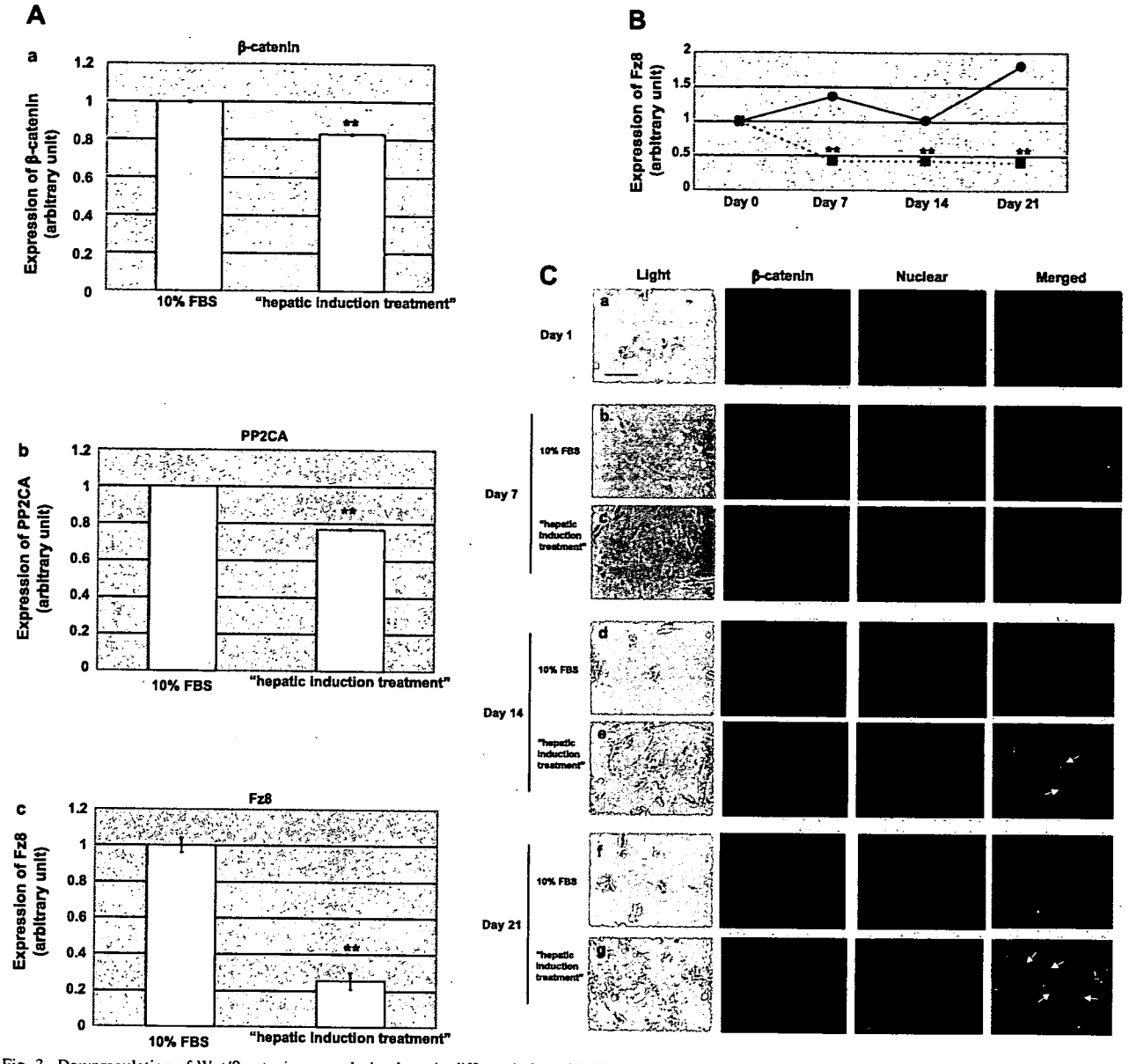

Fig. 3. Downregulation of Wnt/β-catenin genes during hepatic differentiation of UCBTERT-21 cells. *A*: mRNA levels of Wnt/β-catenin signaling genes at *day 21* of control and 5-aza/HGF/OSM/FGF2 treatment as assessed by real-time RT-PCR. Expression levels of the β-catenin (*a*), PP2CA (*b*), and Fz8 (*c*) genes are expressed as a ratio of the control treatment. Data are expressed as means ± SE of 3 experiments. $^{**}P < 0.01$, compared with control. *B*: expression of Fz8 mRNA on *days 0, 7, 14,* and *21* was assessed by real-time RT-PCR. The level of Fz8 is expressed as a ratio of that on *day 0*. ●, 10% FBS (control); ■; 5-aza/HGF/OSM/FGF2. Data are expressed as means ± SE of 3 experiments. $^{**}P < 0.01$, compared with control. *C*: localization of β-catenin in UCBTERT-21 cells during hepatic differentiation. *a, b, d,* and *f*, 10% FBS (control); *c, e,* and *g*, 10% FBS with 5-aza/HGF/OSM/FGF2. Light micrograph (Light), β-catenin staining (β-catenin), nuclear staining (Nuclear), and merged images of β-catenin and nuclear staining (Merged) are shown. SYTOX green was utilized for nuclear staining. β-Catenin was located in the cytoplasm (arrows) of several differentiated cells. Scale bar, 100 μm.

cient induction treatment, tissue engineers might apply this protocol to primary cultured human MSCs, which have not been genetically manipulated.

Recent studies have demonstrated that the Wnt/β-catenin signal plays a crucial role in the regulation of stem cell functions (17). Wnt signaling maintains the self-renewing properties of hematopoietic stem cells and pluripotency of embryonic stem cells (37, 39). In addition to promoting the proliferation of stem/progenitor cells, Wnt also influences the lineage adopted by stem cells. A requirement for Wnt signaling was observed for neuronal specification in the dorsal spinal cord (33). β-Catenin-deficient mouse stem cells fail to differentiate into follicular keratinocytes and instead adopt an epidermal fate (12).

The expression of the gene encoding a Wnt antagonist, Secreted frizzled-related protein 5 (sFRP5), in the foregut endoderm gave rise to the liver in mouse and *Xenopus* (10, 35), suggesting that the Wnt signal is a negative regulator of hepatic

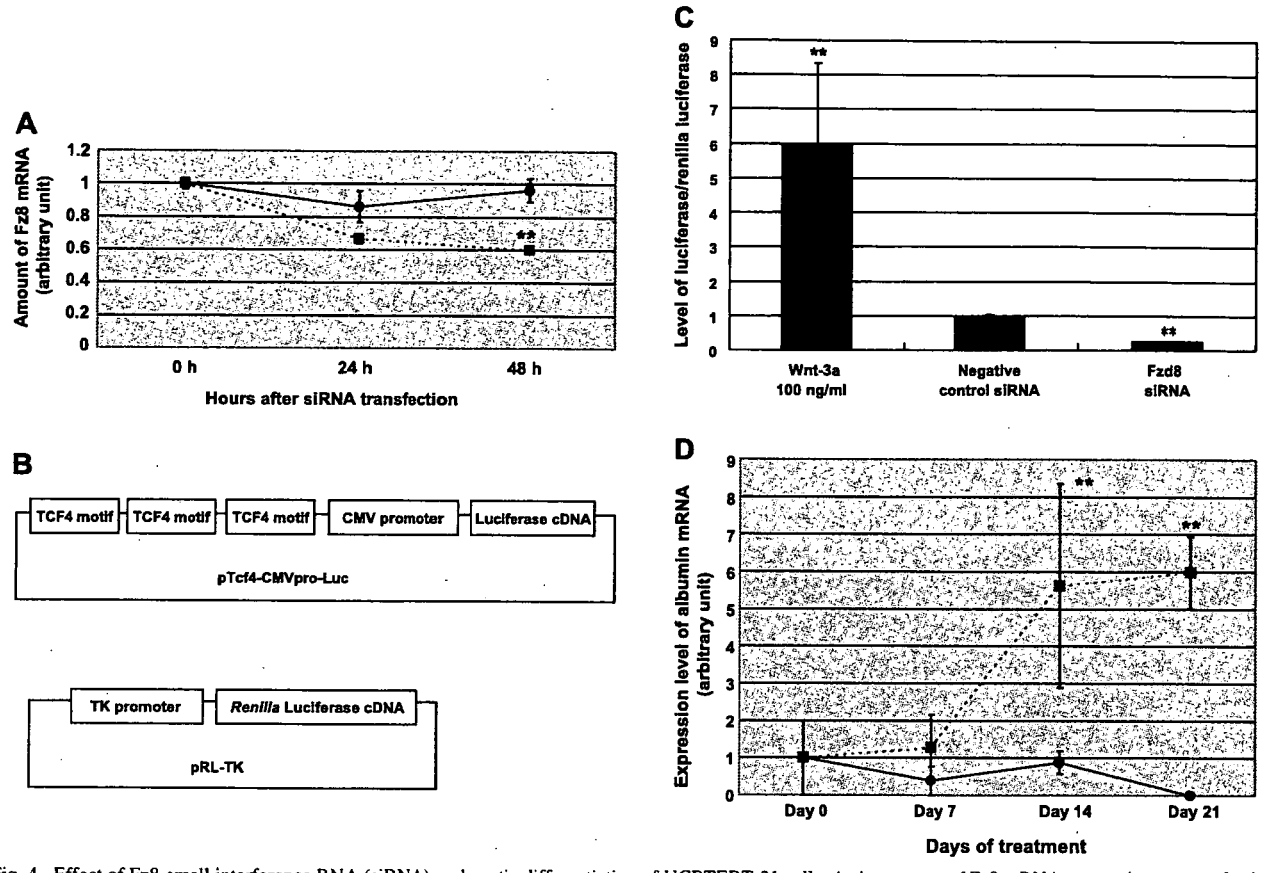

Fig. 4. Effect of Fz8-small interference RNA (siRNA) on hepatic differentiation of UCBTERT-21 cells. *A*: time course of Fz8 mRNA expression on transfection of Fz8-siRNA. The mRNA level of Fz8 was measured by real-time RT-PCR. The level of fzd8 was expressed as a ratio of that at 0 h. ●, negative control siRNA; ■, Fz8-siRNA. Data are expressed as means ± SE of 3 experiments. $^{**}P < 0.01$, compared with the negative control siRNA. *B*: construction of plasmids for the β-catenin-Tcf reporter gene assay. The plasmid contained 3 copies of the optimal Tcf motif upstream of the CMV promoter driving luciferase expression (Tcf4-CMVpro-Luc). A plasmid with the thymidine kinase promoter driving *Renilla* luciferase expression (pRL-TK) was used as an internal control. *C*: reduction of transactivational properties of β-catenin-Tcf4 in UCBTERT-21 cells transfected with fz8-siRNA. The activation level of β-catenin-Tcf4 was expressed as a ratio of that of the negative control siRNA. The level of luciferase activity was examined at 48 h after transfection of pTcf4-CMVpro-luc, pRL-TK, and Fz8-siRNA. The data are expressed as a ratio to *Renilla* luciferase activity. The data from the addition of 100 ng/ml Wnt-3a at 24 h after transfection served a positive control. Data are expressed as means ± SE of 6 experiments. $^{**}P < 0.001$, compared with negative control siRNA. *D*: expression of the albumin gene was induced by Fz8-siRNA transfection. The level of albumin, as evaluated by real-time RT-PCR, was expressed as a ratio of that on *day 0*. ●, negative control siRNA; ■, Fz8-siRNA. Data are expressed as means ± SE of 3 experiments. $^{**}P < 0.01$, compared with *day 0*. *Fig. 4 (Continues).*

development (26). In addition, nuclear β-catenin staining was not observed in hepatocytes from human autopsied tissues at gestational ages 10, 15, 16, 18, 22, and 35 wk (8). Recently, it has been reported that repression of Wnt/β-catenin signaling in the anterior endoderm is essential for development (32). Additional reports have shown a requirement for Wnt signaling after liver cells are formed and not at the time of endoderm specification to form the liver (3, 43). These reports support the results of the present study. In addition, a report that the combination of Wnt and other hepatic growth factors plays an important role in early liver development (13) is in agreement with the present study. It has been recently reported that mesodermal Wnt2b signaling positively regulates liver specification although the species used were different from the present study (34). Differences may arise as to how canonical Wnts can fulfill diverse functions in stem cell. The fact that stem cells from different locations interpret Wnt in different ways obviously reflects an activation of distinct genetic programs in response to the same signal. Although cyclin D1 and c-*myc* are direct target genes of β-catenin/Lef during cell cycle progression, recent studies revealed that proneural genes, neurogenins, are also targets of β-catenin/TCF/Lef during neurogenesis (11, 14). Thus the activation of specific sets of Wnt target genes is likely to be mediated by cell type-specific intrinsic properties. Besides the cell-intrinsic cues that influence the biological activity of Wnt in distinct stem and progenitor cell types, the same type of stem cell might respond in different ways to Wnts, depending on its extracellular microenvironment (17). In this model, Wnt signaling interacts with signaling pathways triggered by other cues and is involved in cross talk with other signals at several levels. Taken together, downregulation of the Wnt/β-catenin pathway plays an important role in the transdifferentiation of MSCs into hepatocytes in response to mesenchymal cell-specific intrinsic properties or cross talk between several cytokines.

In conclusion, we found that the downregulation of Wnt/β-catenin signals play an important role in hepatic differentiation of human UCBMSCs. During hepatic differentiation, Wnt/β-

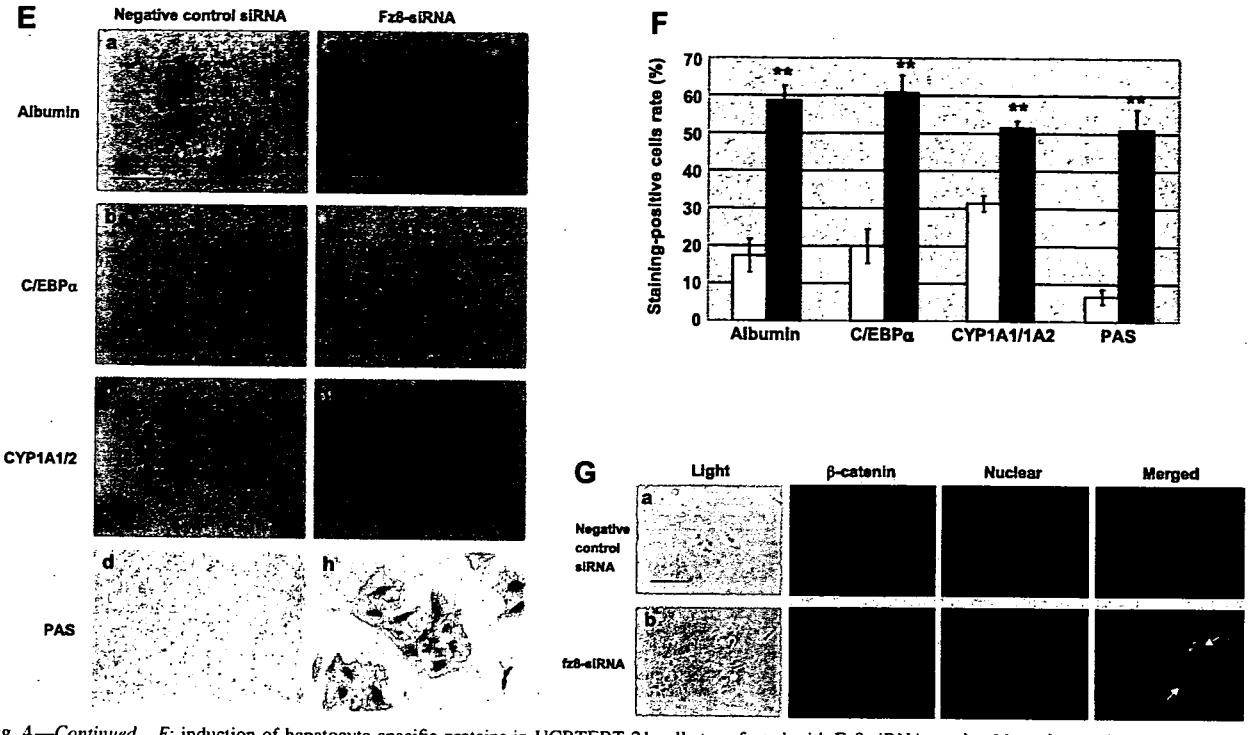

Fig. 4—*Continued.* *E*: induction of hepatocyte-specific proteins in UCBTERT-21 cells transfected with Fz8-siRNA on *day 21*. *a–d*, negative control siRNA; *e–h*, Fz8-siRNA. Cells were immunostained with anti-albumin (*a*, *e*), anti-C/EBPα (*b*, *f*), and anti-CYP1A1/1A2 (*c*, *g*) antibodies. Glycogen stored in cells was stained by PAS stain (*d*, *h*). Scale bar, 100 μm. *F*: efficiency of hepatic differentiation of UCBTERT-21 cells with fzd8-siRNA. Open bars, negative control siRNA; solid bars, Fz8-siRNA. Data are expressed as means ± SE of 6 experiments. $^{**}P < 0.001$ compared with negative control siRNA. *G*: localization of β-catenin in UCBTERT-21 cells transfected with Fz8-siRNA. *a*: Negative control siRNA on *day 21*. *b*: Fz8-siRNA on *day 21*. Light micrograph (Light), β-catenin staining (β-catenin), nuclear staining (Nuclear), and merged images of β-catenin and nuclear staining (Merged) are shown. SYTOX green was utilized for nuclear staining. β-Catenin was located in the cytoplasm (arrows) of several differentiated cells. Scale bar, 100 μm.

catenin signaling was downregulated. Conversely, suppression of the signaling stimulated the hepatic differentiation of UCBTERT-21 cells. These findings provide useful information on stem cell biology, which should contribute to the development of regenerative medicine for liver diseases.

REFERENCES

1. **Alison MR, Poulsom R, Jeffery R, Dhillon AP, Quaglia A, Jacob J, Novelli M, Prentice G, Williamson J, Wright NA.** Hepatocytes from non-hepatic adult stem cells. *Nature* 406: 257, 2000.
2. **Alvarez-Dolado M, Pardal R, Garcia-Verdugo JM, Fike JR, Lee HO, Pfeffer K, Lois C, Morrison SJ, Alvarez-Buylla A.** Fusion of bone marrow-derived cells with Purkinje neurons, cardiomyocytes and hepatocytes. *Nature* 425: 968–973, 2003.
3. **Apte U, Zeng G, Thompson MD, Muller P, Micsenyi A, Cieply B, Kaestner KH, Monga SPS.** β-Catenin is critical for early postnatal liver growth. *Am J Physiol Gastrointest Liver Physiol* 292: G1578–G1685, 2007.
4. **Cadigan KM, Liu YI.** Wnt signaling: complexity at the surface. *J Cell Sci* 119: 395–402, 2006.
5. **Cerec V, Glaise D, Garnier D, Morosan S, Turlin B, Drenou B, Gripon P, Kremsdorf D, Guguen-Guillouzo C, Corlu A.** Transdifferentiation of hepatocyte-like cells from the human hepatoma HepaRG cell line through bipotent progenitor. *Hepatology* 45: 957–967, 2007.
6. **Cerny J, Quesenberry PJ.** Chromatin remodeling and stem cell theory of relativity. *J Cell Physiol* 201: 1–16, 2004.
7. **D'Ippolito G, Schiller PC, Ricordi C, Roos BA, Howard GA.** Age-related osteogenic potential of mesenchymal stromal stem cells from human vertebral bone marrow. *J Bone Miner Res* 14: 1115–1122, 1999.
8. **Eberhart CG, Argani P.** Wnt signaling in human development: beta-catenin nuclear translocation in fetal lung, kidney, placenta, capillaries, adrenal, and cartilage. *Pediatr Dev Pathol* 4: 351–357, 2001.
9. **Fausto N.** Liver regeneration and repair: hepatocytes, prognostic cells, and stem cells. *Hepatology* 39: 1477–1487, 2004.
10. **Finley KR, Tennessen J, Shawlot W.** The mouse secreted frizzled-related protein 5 gene is expressed in the anterior visceral endoderm and foregut endoderm during early post-implantation development. *Genes Expr Patterns* 3: 681–684, 2003.
11. **Hirabayashi Y, Itoh Y, Tabata H, Nakajima K, Akiyama T, Masuyama N, Gotoh Y.** The Wnt/β-catenin pathway directs neuronal differentiation of cortical neural precursor cells. *Development* 131: 2791–2801, 2004.
12. **Huelsken J, Vogel R, Erdmann B, Cotsarelis G, Birchmeier W.** β-Catenin controls hair follicle morphogenesis and stem cell differentiation in the skin. *Cell* 105: 533–545, 2001.
13. **Hussain SZ, Sneddon T, Tan X, Micsenyi A, Michalopoulos GK, Monga SP.** Wnt impacts growth and differentiation in ex vivo liver development. *Exp Cell Res* 292: 157–169, 2004.
14. **Israsena N, Hu M, Fu W, Kan L, Kessler JA.** The presence of FGF2 signaling determines whether β-catenin exerts effects on proliferation or neural differentiation of neural stem cells. *Dev Biol* 268: 220–231, 2004.
15. **Jiang Y, Jahagirdar BN, Reinhardt RL, Schwartz RE, Keene CD, Ortiz-Gonzalez XR, Reyes M, Lenvik T, Lund T, Blackstad M, Du J, Aldrich S, Lisberg A, Low WC, Largaespada DA, Verfaillie CM.** Pluripotency of mesenchymal stem cells derived from adult marrow. *Nature* 418: 41–49, 2002.
16. **Jung J, Zheng M, Goldfarb M, Zaret KS.** Initiation of mammalian liver development from endoderm by fibroblast growth factors. *Science* 284: 1998–2003, 1999.
17. **Kleber M, Sommer L.** Wnt signaling and the regulation of stem cell function. *Curr Opin Cell Biol* 16: 681–687, 2004.
18. **Koh LP, Chao NJ.** Umbilical cord blood transplantation in adults using myeloablative and nonmyeloablative regimens. *Biol Blood Marrow Transplant* 10: 1–22, 2004.

19. **Kondo T.** Epigenetic alchemy for cell fate conversion. *Curr Opin Genet Develop* 16: 1–6, 2006.
20. **Korbling M, Katz RL, Khanna A, Ruifrok AC, Rondon G, Albitar M, Champlin RE, Estrov Z.** Hepatocytes and epithelial cells of donor origin in recipients of peripheral-blood stem cells. *N Engl J Med* 346: 738–746, 2002.
21. **Krause DS, Theise ND, Collector MI, Henegariu O, Hwang S, Gardner R, Neutzel S, Sharkis SJ.** Multi-organ, multi-lineage engraftment by a single bone marrow-derived stem cell. *Cell* 105: 369–377, 2001.
22. **Lagasse E, Connors H, Al-Dhalimy Reitsma M, Dohse M, Osborne L, Wang X, Finegold M, Weissman IL, Grompe M.** Purified hematopoietic stem cells can differentiate into hepatocytes in vivo. *Nat Med* 6: 1229–1234, 2000.
23. **Lakshmipathy U, Verfaillie C.** Stem cell plasticity. *Blood Rev* 19: 29–38, 2005.
24. **Lee KD, Kuo TK, Wang-Peng J, Chung YF, Lin CT, Chou SH, Chen JR, Chen YP, Lee OK.** In vitro hepatic differentiation of human mesenchymal stem cells. *Hepatology* 40: 1275–1284, 2004.
25. **Lee OK, Kuo TK, Chen WM, Lee KD, Hsieh SL, Chen TH.** Isolation of multipotent mesenchymal stem cells from umbilical cord blood. *Blood* 103: 1669–1675, 2004.
26. **Lemaigre F, Zaret KS.** Liver development update: new embryonic models, cell lineage control, and morphogenesis. *Curr Opin Genet Dev* 14: 582–590, 2004.
27. **Li X, Yost HJ, Virshup DM, Seling JM.** Protein phosphatase 2A and its B56 regulatory subunit inhibit Wnt signaling in Xenopus. *EMBO J* 20: 4122–4131, 2001.
28. **Lu FZ, Fujino M, Kitazawa Y, Uyama T, Hara Y, Funeshima N, Jiang JY, Umezawa A, Li XK.** Characterization and gene transfer in mesenchymal stem cells derived from human umbilical-cord blood. *J Lab Clin Med* 146: 271–278, 2005.
29. **Makino S, Fukuda K, Miyoshi S, Konishi F, Kodama H, Pan J, Sano M, Takahashi T, Hori S, Abe H, Umezawa A, Ogawa S.** Cardiomyocytes can be generated from marrow stromal cells in vitro. *J Clin Invest* 103: 697–705, 1999.
30. **Mayani H, Lansdorp PM.** Biology of human umbilical cord blood-derived hematopoietic stem/progenitor cells. *Stem Cells* 16: 153–165, 1998.
31. **Micsenyi A, Tan X, Sneddon T, Luo J, Michalopoulos GK, Monga SPS.** β-Catenin is temporally regulated during normal liver development. *Gastroenterology* 126: 1134–1146, 2004.
32. **McLin VA, Rankin SA, Zorn A.** Repression of Wnt/β-catenin signaling in the anterior endoderm is essential for liver and pancreas development. *Development* 134: 2207–217, 2007.
33. **Muroyama Y, Fujihara M, Ikeya M, Kondoh H, Takada S.** Wnt signaling plays an essential role in neuronal specification of the dorsal spinal cord. *Genes Dev* 16: 548–553, 2002.
34. **Ober EA, Verkade H, Field HA, Satinier DY.** Mesodermal Wnt2b signalling positively regulates liver specification. *Nature* 442: 688–691, 2006.
35. **Pilcher KE, Krieg PA.** Expression of the Wnt inhibitor, sFRP5, in the gut endoderm of Xenopus. *Gene Expr Patterns* 2: 369–372, 2002.
36. **Ratcliffe MJ, Itoh K, Sokol SY.** A positive role for the PP2A catalytic subunit in Wnt signal transduction. *J Biol Chem* 175: 35680–35683, 2000.
37. **Reya T, Duncan AW, Alles L, Domen J, Scherer DC, Willert K, Hintz L, Nusse R, Weissman IL.** A role for Wnt signalling in self-renewal of haematopoietic stem cells. *Nature* 423: 409–414, 2003.
38. **Roose J, Huls G, Beest von M, Moerer P, van der Horn K, Goldschmeding R, Logtenberg T, Clevers H.** Synergy between tumor suppressor APC and the b-catenin-Tcf4 target Tcf1. *Science* 285: 1923–1926, 1999.
39. **Sato N, Meijer L, Skaltsounis L, Greengard P, Brivanlou AH.** Maintenance of pluripotency in human and mouse embryonic stem cells through activation of Wnt signaling by a pharmacological GSK-3-specific inhibitor. *Nat Med* 10: 55–63, 2004.
40. **Schmidt C, Bladt F, Goedecke S, Brinkmann V, Zschiesche W, Sharpe M, Gherardi E, Birchmeier C.** Scatter factor/hepatocyte growth factor is essential for liver development. *Nature* 373: 699–702, 1995.
41. **Schwartz RE, Reyes M, Koodie L, Jiang Y, Blackstad M, Lund T, Lenvik T, Johnson S, Hu WS, Verfaillie CM.** Multipotent adult progenitor cells from bone marrow differentiate into functional hepatocyte-like cells. *J Clin Invest* 109: 1291–1302, 2002.
42. **Shiota G, Okano J, Kawasaki H, Kawamoto T, Nakamura T.** Serum hepatocyte growth factor levels in liver diseases: clinical implications. *Hepatology* 21: 106–112, 1995.
43. **Suksawaeng S, Lin CM, Jiang TX, Hughes MW, Widelitz RB, Chuong CM.** Morphogenesis of chicken liver: identification of localized growth zones and the role of β-catenin/Wnt in size regulation. *Development* 266: 109–122, 2004.
44. **Tago K, Nakamura T, Nishita M, Hyodo J, Nagai S, Murata Y, Adachi S, Ohwada S, Morishita Y, Shibuya H, Akiyama T.** Inhibition of Wnt signaling by ICAT, a novel β-catenin-interacting protein. *Genes Dev* 14: 1741–1749, 2000.
45. **Tanabe Y, Tajima F, Nakamura Y, Shibasaki E, Wakejima M, Shimomura T, Murai R, Murawaki Y, Hashiguchi K, Kanbe T, Saeki T, Ichiba M, Yoshida Y, Mitsunari M, Yoshida S, Miake J, Yamamoto Y, Nagata N, Harada T, Kurimasa A, Hisatome I, Terakawa N, Murawaki Y, Shiota G.** Analyses of clarify rich fractions in hepatic progenitor cells from human umbilical cord blood and cell fusion. *Biochem Biophys Res Commun* 324: 711–718, 2004.
46. **Terai M, Uyama T, Sugiki T, Li XK, Umezawa A, Kiyono T.** Immortalization of human fetal cells: the life span of umbilical cord blood-derived cells can be prolonged without manipulating $p16^{INK4a}$/RB braking pathway. *Mol Biol Cell* 16: 1491–1499, 2005.
47. **Theise ND, Nimmmakakalu M, Gardner R, Illei PB, Morgan G, Teperman L, Henegariu O, Krause DS.** Liver from bone marrow in human. *Hepatology* 31: 235–240, 2000.
48. **Zaret KS.** Genetic control of hepatocyte differentiation. In: *The Liver* (3rd ed.), edited by Arias IM, Boyer JL, Fausto N, Jakoby WB, Schachter D, and Shafritz DA. New York: Raven, 1994, p. 53–68.

Available online at www.sciencedirect.com
ScienceDirect
Biochemical and Biophysical Research Communications 364 (2007) 838–843
BBRC
www.elsevier.com/locate/ybbrc

Preferential localization of SSEA-4 in interfaces between blastomeres of mouse preimplantaion embryos

Ban Sato [a,e], Yohko U. Katagiri [a,d,*], Kenji Miyado [b], Hidenori Akutsu [b], Yoshitaka Miyagawa [a], Yasuomi Horiuchi [a], Hideki Nakajima [a], Hajime Okita [a,d], Akihiro Umezawa [b], Jun-ichi Hata [a], Junichiro Fujimoto [c,d,1], Kiyotaka Toshimori [e], Nobutaka Kiyokawa [a,d]

[a] *Department of Developmental Biology, National Research Institute for Child Health and Development, 2-10-1 Okura, Setagaya-ku, Tokyo 157-8535, Japan*
[b] *Department of Reproductive Biology, National Research Institute for Child Health and Development, 2-10-1 Okura, Setagaya-ku, Tokyo 157-8535, Japan*
[c] *National Research Institute for Child Health and Development, 2-10-1 Okura, Setagaya-ku, Tokyo 157-8535, Japan*
[d] *Core Research for Evolutional Science and Technology (CREST) of Japan Science and Technology Corporation (JST), Japan*
[e] *Department of Anatomy and Developmental Biology, Graduate School of Medicine, Chiba University, Chiba 260-8670, Japan*

Received 11 October 2007
Available online 26 October 2007

Abstract

The monoclonal antibody 6E2 raised against the embryonal carcinoma cell line NCR-G3 had been shown to also react with human germ cells. Thin-layer chromatography (TLC) immunostaining revealed that 6E2 specifically reacts with sialosylglobopentaosylceramide (sialylGb5), which carries an epitope of stage-specific embryonic antigen-4 (SSEA-4), known as an important cell surface marker of embryogenesis. The immunostaining of mouse preimplantation embryos without fixation showed that the binding of 6E2 caused the clustering and consequent accumulation of sialylGb5 at the interface between blastomeres. These results suggest that SSEA-4 actively moves on the cell surface and readily accumulates between blastomeres after binding of 6E2.

Keywords: SialylGb5; SSEA-4; Embryonic stem cells; Embryonal carcinoma cells; Preimplantation embryo; Immunostaining

Embryonal carcinoma (EC) cells isolated from teratocarcinomas have been shown to possess pluri- or multipotency in both mouse and human systems [1–3]. In mice, certain EC cells as well as embryonic stem (ES) cells have been considered to be developmentally equivalent to the inner cell mass of blastocysts [1]. These EC cells are useful for clarifying the molecular characteristics of early embryonic cells and thus many efforts have been made to establish EC cell lines and monoclonal antibodies (Mabs) that detect differentiation-related molecules on EC cells. As a consequence, a number of stage-specific markers for embryogenesis have been identified. Notably, it is important that this molecular information is adapted to research on ES cells or mouse preimplantation embryos. Stage-specific embryonic antigen (SSEA) -1, -3, and -4, as well as tumor rejection antigen (TRA) -1-60 and -1-81 [4], have been used as stage-specific markers for embryogenesis, though their functional significance in early development remains unclear. Interestingly, however, most of these antigens are carbohydrates themselves or closely related to the carbohydrates carried on glycosphingolipids (GSLs) and glycoproteins [5].

6E2 is a Mab established by immunizing with NCR-G3 cells, a previously established multipotent human EC cell

* Corresponding author. Address: Department of Developmental Biology, National Research Institute for Child Health and Development, 2-10-1 Okura, Setagaya-ku, Tokyo 157-8535, Japan. Fax: +81 3 3417 2496.
E-mail address: kata@nch.go.jp (Y.U. Katagiri).
[1] Vice General Director.

0006-291X/$ - see front matter © 2007 Elsevier Inc. All rights reserved.
doi:10.1016/j.bbrc.2007.10.093

line capable of differentiating into trophoblastic cell lineages other than somatic cells [3]. It has been revealed that 6E2 reacts with not only human ECs, including NCR-G2 and 3 cells, but also other germ cell tumors, as well as normal human germ cells such as spermatogonia and oocytes [6]. Although a previous study reported that 6E2 immunoprecipitates a cell surface protein having a molecular weight of approximately 80 kDa from ^{125}I-labeled NCR-G3 cells, the specific antigen recognized by 6E2 still remains unknown. To characterize the antigen specificity of 6E2, we examined the reactivity of the Mab with other cell lines using several distinct methods. In this paper, we present evidence that 6E2 recognizes SSEA-4 carried by sialylGb5. Using 6E2, we determined the localization of SSEA-4 in "living" mouse preimplantation embryos and observed its preferential localization in interface between blastomeres.

Materials and methods

Cells, antibodies, and animals. The human renal carcinoma cell line ACHN was purchased from American Type Culture Collection. The African green monkey kidney cell line Vero was a gift from Dr. T. Takeda of Department of Infectious Diseases Research, National Children's Medical Research Center, Tokyo, Japan. Cells were maintained in Dulbecco's modified Eagle's minimum essential medium (DMEM) (Sigma Chem., St. Louis, MO) supplemented with 10% fetal bovine serum (FBS) (JRH Bioscience, Lenexa, KS). The human EC cell line NCR-G2 [3] was cultured in a 1:1 mixture of DMEM and Ham's F12 medium (DMEM/F12) (Invitrogen Gibco, Carlsbad, CA) supplemented with 10% FBS(JRH Bioscience), non-essential amino acid solution (NEAA) (Invitrogen Gibco), and Insulin-Transferin-Sodium Selenite media (Invitrogen Gibco). The cynomolgus monkey ES cell line CMK-6 [7] were provided by Dr. Yasushi Kondo of Mitsubishi Tanabe Pharma Corporation. ES cells were grown on mouse embryonic fibroblast feeder cells that were inactivated by gamma-irradiation in DMEM/F12 supplemented with 20% Knockout™ Serum Replacement, 2 mM Glutamax-I, 1% NEAA, 50 units/ml penicillin, 50 μg/ml streptomycin, 0.1 mM 2-mercaptoethanol, 1% sodium pyruvate, and 5 ng/ml bFGF (all from Invitrogen GIBCO). The cultures were performed at 37 °C in a 5% CO_2 incubator. The human venous blood from a healthy consenting volunteer was drawn in a heparin-coated syringe. The blood was spun at 3000 rpm for 15 min and human red blood cells (hRBCs) were washed three times in phosphate buffered saline (PBS).

The conjugation of affinity-purified 6E2 (mouse IgG_3, κ) [6] to the fluorescence reagent was performed with an Alexa Fluor® 488 monoclonal antibody labeling kit (Molecular Probes, Eugene, OR.) according to the manufacturer's instructions. The anti-SSEA-4 Mabs used in this study were Raft.2 [8] and MC813-70 (R&D Systems, Inc Minneapolis, MN). Alexa Fluor® 488 goat anti-mouse IgG and Streptavidin Alexa Fluor® 568 were purchased from Molecular probes.

BDF_1 mice were purchased from Clea Japan (Tokyo, Japan).

TLC immunostaining of GSLs. TLC immunostaining of GSLs from cultured cells and hRBCs was performed as previously described [9]. Reference GSLs were purchased from Matlayer, Inc. (Pleasant Gap, PA). SialylGb5 was purified from ACHN cells by preparative TLC. Purified GM1 b was kindly provided by Dr. Nakamura of RIKEN, Saitama, Japan [10].

Flow cytometry. Cells were harvested and incubated with a primary antibody (1 μg/ml) for 1 h on ice, followed by treatment with fluorescein isothiocyanate-conjugated goat anti-mouse immunoglobulins (Jackson Immunoresearch Laboratories, Inc., West Grove, PA) at a dilution of 1:50 and analyzed with an EPICS-XL flow cytometer (Beckman Coulter, Inc, Miami, FL).

Dot blot analysis. Purified sialylGb5 was serially diluted (0.1–60 ng) and vacuum blotted onto a PVDF membrane by using a 96-well format dot blot apparatus (Bio-Rad Laboratories, Richmond, CA). The membrane was immunostained with the Mab 6E2 or MC813-70 (0.5 μg/ml) according to a previously described procedure [9]. The antibodies that bound to the membranes were visualized with ECL-plus Western Blotting Detection Reagents (GE Healthcare UK Ltd, Buckinghamshire, UK) and scanned with a LAS-1000 luminescent imaging analyzer (Fujifilm, Tokyo, Japan). Scanned images were analyzed using the software Image Gauge with which the LAS-1000 was equipped.

Indirect immunostaining of cynomolgus monkey ES cells. Cells were grown on a glass-bottomed dish (IWAKI) for 3 days and then these cells were fixed for 30 min with 4% paraformaldehyde in PBS and permeabilized with 0.2% Triton X-200 in PBS for 20 min. Subsequently, the cells were washed three times with PBS for 5 min and blocked with 5% normal goat serum in PBS for 30 min. The fixed cells were incubated with anti-SSEA-4 antibodies or isotype-matched mouse IgG at a dilution of 1:300 for 2 h, followed by incubation with Alexa Fluor® 488-conjugated goat anti-mouse IgG at a dilution of 1:300 for 30 min. DAPI was used for counter staining of nuclei.

Immunostaining of mouse preimplantation embryos. Mouse preimplantation embryos were collected from superovulated mice. Seven-week-old BDF1 female mice were induced to superovulate with intraperitoneal injections of pregnant mare's serum gonadotropin (ASKA Pharmaceutical co., Ltd., Tokyo, Japan) (5 IU) and human chorionic gonadotropin (hCG) (ASKA Pharmaceutical co) (5 IU) 48 h apart and mated with individual BDF1 male mice after the hCG injection. The 2-cell, the 8-cell, and the morula stage embryos were flushed out from oviducts at 36, 60, and 72 h after the hCG injection, respectively. Animals were treated according to the institutional animal care and use guidelines of National Research Institute for Child Health and Development.

Embryos immediately after being collected and those prefixed with 2% paraformaldehyde in Hepes buffered saline were incubated in 30 μl drops of M16 medium containing 0.45 μg of Alexa Fluor® 488-conjugated 6E2 for 1 h or biotinylated MC813-70 for 1 h, treated with streptavidin Alexa Fluor® 568 diluted 1:300, and then they were washed three times in 30 μl drops of M16 medium. All staining steps were carried out at 37 °C in a CO_2 incubator for fresh embryos and at 4 °C for fixed embryos. The stained embryos were placed in drop of a M16 medium on glass-bottomed dishes (IWAKI, Tokyo, Japan), and were observed with a LSM510 Zeiss Confocal laser-scanning microscope (Carl Zeiss, Thornwood, NY) to obtain a field of view of the embryo only with a 40× objective lens.

Results and discussion

6E2 specifically binds to sialylGb5

In order to examine whether the 80 kDa membrane protein is recognized by 6E2, we performed a Western analysis of the cell lysates or their immunoprecipitates with 6E2. Since no significant signal was detected on the blot (data not shown), we examined TLC immunostaining of GSLs extracted from several 6E2-positive cell lines. ACHN cells showed the expression of comparable amounts of Gb3, Gb4, Gb5, and sialylGb5, whereas Vero cells and NCR-G2 cells expressed predominantly Gb3 (Fig. 1A). TLC immunostaining analysis revealed that 6E2 binds to a major slow-migrating GSL extracted from these three cell lines. The slow-migrating GSL was identified as sialylGb5, defined by the Mab Raft.2. We observed that 6E2 bound to sialylGb5 (LKE-antigen) of hRBCs [13] (Fig. 1B). Finally, we examined the reactivity of 6E2 with purified GSLs and found that the Mab reacts with purified sialylGb5, but not purified GM1 b (Fig. 1C). These results indicate that 6E2 specifically binds to sialylGb5 and thus is an anti-SSEA-4